Available online at www.sciencedirect.com
SCIENCE DIRECT
Precambrian Research 131 (2004) 73–109
Precambrian Research
www.elsevier.com/locate/precamres

# Timing and evolution of multiple Paleoproterozoic magmatic arcs in the Tapajós Domain, Amazon Craton: constraints from SHRIMP and TIMS zircon, baddeleyite and titanite U–Pb geochronology

João Orestes S. Santos [a,d,*], Otto B. Van Breemen [b], David I. Groves [c], Léo A. Hartmann [d], Marcelo E. Almeida [a], Neal J. McNaughton [c], Ian R. Fletcher [c]

[a] Geological Survey of Brazil, Rua Banco Província 105, Porto Alegre, RS 90840-030, Brazil
[b] Geological Survey of Canada, 601 Booth Street, Ottawa, Ont., Canada K1A 0E8
[c] Centre for Global Metallogeny, University of Western Australia, Crawley, WA 6009, Australia
[d] Instituto de Geociências, Universidade Federal do Rio Grande do Sul, Av. Bento Gonçalves 9500, Porto Alegre, RS 91501-970, Brazil

Received 10 July 2003; accepted 16 January 2004

**Abstract**

Knowledge of the geotectonic evolution of the Tapajós Domain of the Tapajós–Parima Orogen is of major significance in the Amazon Craton, for two reasons: first, the domain lies between the Archean Central Amazon Province to the east-northeast and the Paleo–Mesoproterozoic Juruena Province (1820–1520 Ma) to the southwest and, second, it has produced a large proportion of Brazilian gold in the last century. Geological mapping, integrated with U–Pb zircon, baddeleyite and titanite SHRIMP and TIMS geochronology, shows that the Tapajós Domain is a complex array of plutonic and volcanic rock associations formed during two main events: the Tapajós–Parima Orogen (2040–1880 Ma) and a later post-orogenic period (1870–1760 Ma). Whole-rock and zircon geochemistry help discriminate both the more primitive from the more evolved orogenic rocks and the anorogenic rocks from the arc-related magmatism. In contrast with previous model, whereby the Orosirian Tapajós–Parima Orogen was interpreted to have resulted from one orogeny involving three magmatic arcs, this new interpretation shows that the orogen developed during two distinct orogenies and incorporates five magmatic arcs. The two orogenies, Mundurucus (2040–1957 Ma) and Tropas (1906–1886 Ma) are separated by a hiatus of about 50 million years. The Mundurucus Orogeny started with island arc magmatism (banded tonalite, meta-basalt and meta-andesite, Cuiú–Cuiú Complex; 2040–1998 Ma) and turbiditic sedimentation in back-arc or trench basins (Jacareacanga Group) followed by the formation of two Andean-type continental arcs composed of syeno- and monzogranites and felsic to intermediate volcanic rocks (Jamanxim; 2000–1986 Ma; Creporizão, 1980–1957 Ma). After a hiatus of about 50 million years, the Tropas Orogeny also started with island arc magmatism (Tropas Suite; 1906–1886 Ma), again followed by formation of a third continental arc (Parauari Suite). Contrary to previous interpretations, which included all felsic to intermediate volcanic rocks from the Tapajós Domain in the Iriri Group (1.87 Ga), we now recognize older (2.02–1.88 Ga) orogenic calc-alkaline volcanic rocks in four orogenic arcs. The post-orogenic Uatumã magmatism (Maloquinha Intrusive Suite of granitic rocks and Iriri Group of volcanic rocks) took place at ∼1870 Ma, with another, much younger anorogenic magmatic event represented by the Porquinho Granite (1786 ± 14 Ma) correlated to the Teles Pires Suite. Similarly, some of the intrusive post-orogenic granitic rocks are interpreted to be related to the younger Teles Pires Suite rather than to the Maloquinha Suite.

* Corresponding author. Tel.: +55-51-3235-2420; fax: +55-51-3235-2470.
*E-mail address:* orestes1@uol.com.br (J.O.S. Santos).

0301-9268/$ – see front matter 
doi:10.1016/j.precamres.2004.01.002

Archean ages on inherited zircon, together with Sm–Nd data, provide strong evidence that the post-orogenic rocks were derived from continental Archean crust, possibly from the Central Amazon Province to the east.


*Keywords:* Amazon Craton; Tapajós Domain; Orosirian; U–Pb SHRIMP geochronology; Zircon; Baddeleyite

## 1. Introduction

During the Orosirian, several Archean continents were amalgamated to form the Amazonia and Laurentia supercontinents (Hoffman, 1988; Rogers, 1996). Evidence for ocean shortening and closure is contained within extensive orogenic belts, which include the Trans-Hudson Orogen of Laurentia (Van Schmus et al., 1987; Bickford et al., 1990) and the Tapajós–Parima Orogen of Amazonia (Santos et al., 2000). The Tapajós–Parima Orogen extends for over 2000 km through the Amazon Craton in Brazil (Santos et al., 2000; Hartmann and Delgado, 2001) and is one of the largest preserved Orosirian orogenic belts in the world. It lies west of the supposedly Archean, Central Amazon Province and is largely obscured by a Statherian overprint to the west (Rio Negro and Rondônia-Juruena provinces; Santos et al., 2000). Development of this orogenic system corresponds to a major phase of the Atlantica continent assembly. Prior to this study, the duration and upper and lower age limits of the Tapajós–Parima Orogen were not well-established, nor was the timing of its orogenic events. The Tapajós Domain is an important area to be investigated the ages of orogenic events because it is one of the main gold provinces of Brazil (the main source of gold in Brazil from 1965 to 1992) and hence there are about 300 air-strips open in the jungle to support mining activity. The economic importance of the Domain and the aerial access to remote areas motivated a regional mapping project by the Brazilian Geological Survey (CPRM) and several exploration programs by mining companies, which resulted in thousands of surface and drill core samples for study.

The timing of geological events was previously constrained using samples from widely dispersed sites and Rb–Sr geochronology, whereas the present study has integrated U–Pb geochronology with regional lithological and structural mapping of a broad area within the Tapajós Project of the Brazilian Geological Survey.

The tectonic style, the upper and lower age limits, and the orogenic duration and evolution of the Tapajós Domain are all questions open to investigation. Another question under debate is the possible extension of the Tapajós–Parima Orogen to the Ventuari region of Venezuela (Tassinari, 1996; Tassinari and Macambira, 1999; Tassinari et al., 2000; Payolla et al., 2002).

The objective of this paper is to provide geochronological constraints for the main magmatic events during the evolution of the Tapajós Domain. This paper reports new SHRIMP and TIMS U–Pb data on zircon, titanite and baddeleyite for eight samples of granitoids (six), gabbros (one) and pyroclastic rocks (one) from five different magmatic suites (Jamanxim, Creporizão, Tropas, Parauari and Teles Pires) and reinterprets the existing SHRIMP (Santos et al., 2001), conventional U–Pb (Santos et al., 2000) and Pb–Pb (Klein and Vasquez, 2000; Vasquez and Klein, 2000) zircon age data. The considerable amount of U–Pb data generated in the last few years makes the Tapajós Domain the best documented Paleoproterozoic tectonic unit of the Amazon Craton. Rock major and trace element, compositions are used to discriminate the orogenic suites as well as to compare them with the post-orogenic suites.

## 2. Regional geology and previous geochronology

The region records a long and complex history of evolution of Paleoproterozoic continental crust evolution. This evolution was initially constrained by regional mapping (Pessoa et al., 1977; Bizzinella et al., 1980) and Rb–Sr geochronology (Pessoa et al., 1977; Tassinari, 1996; Tassinari et al., 2000) of a few stratigraphic units. The paucity of data over this large domain led several authors to interpret that the region formed under different tectonic environments in different epochs (Table 1). None of these models are now acceptable.

Several rock samples were dated by the whole-rock Rb–Sr reference isochron method, during the 1975–1982 period (Basei, 1974; Santos et al., 1975; Pessoa et al., 1977; Bizzinella et al., 1980; Santos and

Table 1
Previous ages and tectonic interpretations of the Tapajós Domain

| Tectonic environment | Age | References |
|---|---|---|
| Greenstone belt | Archean to Paleoproterozoic (2.70–1.80 Ga) | Pessoa et al. (1977), Bizzinella et al. (1980), Santos (1984) |
| One magmatic arc | 1.90–1.80 Ga | Tassinari (1996) |
| Collisional belt | Archean to Early Paleoproterozoic | Costa and Hasui (1997) |
| Mobile belt | 2.45–2.25 Ga | Lima (1999) |
| Three magmatic arcs | 2.10–1.88 Ga | Santos et al. (2000) |

Reis Neto, 1982). The Rb–Sr isotopic compositions were affected by partial loss of radiogenic $^{87}Sr$, and nearly all results are 50–350 million years younger than the more reliable Pb–Pb and U–Pb results obtained in the same samples or units during the last 5 years (Santos et al., 1997, 2000). In spite of the concentration of Rb–Sr ages in the 1845–1650 Ma range, several authors considered that the history of the Tapajós region began in the Archean (Santos et al., 1975; Bizzinella et al., 1980; Santos, 1984; Costa and Hasui, 1997). This interpretation appears to have resulted from an incorrect correlation of the Tapajós basement (Cuiú–Cuiú Complex and Jacareacanga Group) to the Archean Xingu Complex in the Carajás Province.

A reliable chronostratigraphy of the Tapajós Domain started to be established since 1997 when zircon, titanite and baddeleyite U–Pb and Pb–Pb isotopic data became available (Santos et al., 1997, 2000, 2001; Klein and Vasquez, 2000; Vasquez and Klein, 2000; Lamarão et al., 2002). This recent U–Pb data set, and new field data (Almeida et al., 2000; Santos et al., 2000), led to the interpretation that part of the Tapajós region (the Tapajós Domain) belongs to the Tapajós–Parima Orogen (Fig. 1), formed between 2.05 and 1.88 Ga (Table 2). This age range of the orogen is post-Trans-Amazonian Cycle (2.26–2.01 Ga; Santos et al., 2003a). The orogenic belt is composed mostly of magmatic arcs, mapped as granitoid suites (Klein and Vasquez, 2000; Santos et al., 2000; Almeida et al., 2000).

There are four distinctive domains in the orogenic belt, separated from each other by three Phanerozoic sedimentary basins (Fig. 1): the Cenozoic Solimões Basin to the north, the Paleozoic–Mesozoic Amazon Basin in the center and the Cachimbo Basin in the south.

Two main terrains dominate Tapajós geology: an orogenic belt to the west and a cratonic assemblage

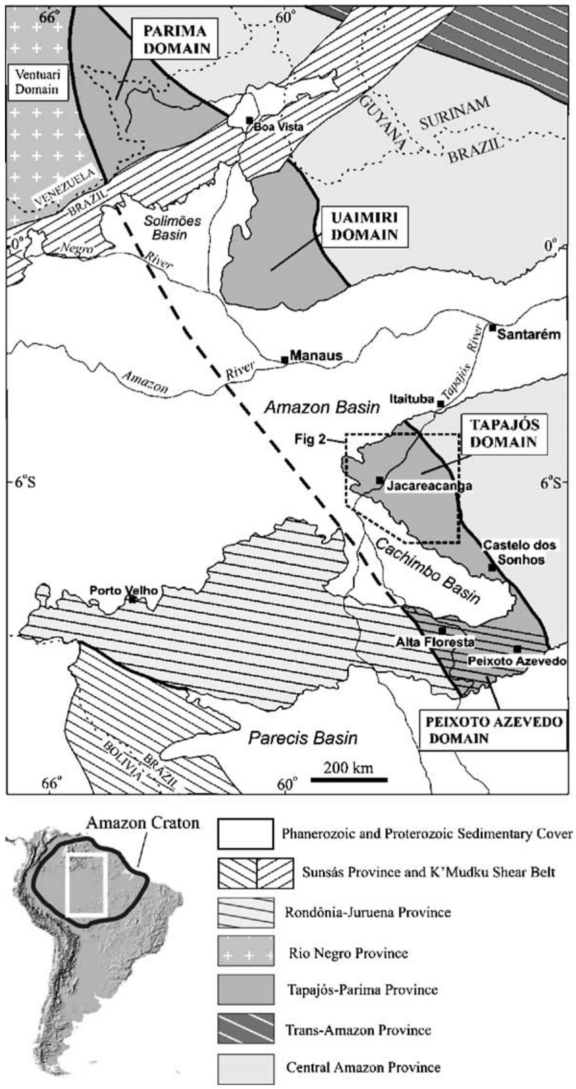


Fig. 1. Geographic location of the four domains of the Tapajós–Parima Orogenic belt.

Table 2
Summary of the Paleoproterozoic rock assemblages of the Tapajós Domain in chronological order

| Stratigraphic unit/tectonic setting | Age (Ma)[a] | Assemblage | Interpretation |
|---|---|---|---|
| Teles Pires Intrusive Suite/cratonic | 1793–1767 | $A_1$-type orthoclase granite, perthite granite and rapakivi granite | Continental rift, mantle plumes |
| Crepori diabase/cratonic | 1789–1771 | Continental tholeiites, gabbro-diabase dikes and sills | Continental rift, mantle plumes |
| Palmares Group/cratonic | >1780; <1870 | Quartz–sandstone, arkose, conglomerate, felsic tuff, pink shale | Continental rift-basin: fluvial braided, alluvial fan and pyroclastic deposits |
| Uatumã Supergroup, Maloquinha Intrusive Suite/post-orogenic | 1877–1864 | $A_2$-type orthoclase granite, perthite granite, granophyre, syenogranite | Underplating |
| Uatumã Supergroup Iriri Group/post-orogenic | 1874–1870 | Rhyodacite, rhyolite, andesite, latite, dacite, tuff, breccia, agglomerate | Underplating |
| Parauari/orogenic | 1885–1877 | Monzogranite, syenogranite, gabbro, anorthosite | Continental arc |
| Tropas/orogenic | 1907–1886 | Tonalite, granodiorite, basalt | Island arc/continental arc |
| Creporizão/orogenic | 1980–1957 | Monzogranite, andesite | Continental arc |
| Cuiú–Cuiú/orogenic | 2040–1998 | Tonalite, basalt | Island arc |
| Jacareacanga Group, Sai-Cinza turbidites/orogenic | 2020–2000 | Turbidite, chert, banded iron formation | Trench and back-arc sedimentation |
| Jacareacanga Group, Tapuru Basalt/orogenic | >2020 | Oceanic basalt | Ocean crust |

[a] All ages are U–Pb (Santos et al., 2001) and Pb–Pb evaporation (Vasquez and Klein, 2000), except the age of the undated Tapuru Basalt. This is inferred from its field relation with the Sai-Cinza Schist.

to the east (Fig. 2). The orogenic belt is composed of a back-arc sequence consisting of turbidites (Sai-Cinza Schist), oceanic basalts (Tapuru Basalt, Jacareacanga Group) and a succession of granitoid suites. The cratonic rocks (Table 2) mostly correspond to the volcano-plutonic Uatumã Supergroup, which is composed of the Iriri Group (rhyolite-andesite volcanic and pyroclastic rocks) and the Maloquinha Intrusive Suite ($A_2$-type granites). Pessoa et al. (1977) and Bizzinella et al. (1980) mapped two main pre-Uatumã granitoid units in the Tapajós region: the Cuiú–Cuiú Complex and the Parauari Intrusive Suite.

### 2.1. Supracrustal rocks

The Jacareacanga Group, a metamorphosed volcano-sedimentary sequence with a north-northwest structural trend exposed in the westernmost part of the orogenic belt (Fig. 2), was thought to be an Archean greenstone belt (Bizzinella et al., 1980). Santos et al. (2000) redefined the Jacareacanga Group as most likely an accretionary sequence, based on the small volume of preserved basalts and the lack of a typical granitoid-greenstone dome-and-keel pattern between the supracrustal rocks and the syn-tectonic granitoids (Cuiú–Cuiú Complex). The group has three main rock associations: (1) an upper turbiditic sequence metamorphosed at greenschist facies conditions (Sai-Cinza Schist)—sericite schist, sericite quartzite and phyllite: this is the dominant lithostratigraphic unit; (2) a metamorphosed chemical sedimentary unit interlayered with the turbidites and composed by chert and beds of banded iron formation; (3) metamorphosed oceanic basalts (actinolite and chlorite schists), which are more abundant in the western part of the belt and interpreted as the basal sequence.

Detrital zircons from the Jacareacanga Group have ages near 2875, 2125, 2106 and 2098 Ma (Sai-Cinza Schist; Santos et al., 1997, 2000) and 2189, 2136, 2034 and 2008 Ma (Espírito Santo Schist; Almeida et al., 2001) and therefore provide information about the pre-Tapajós crust. Zircon ages between 2125 and 2098 Ma may represent the timing of primitive magmatism related to the rifting of the ocean basins. However, the small number of detrital zircon grains analyzed (eight) precludes the establishment of the maximum age of the Jacareacanga Group. It is considered to be older than the Cuiú–Cuiú Complex, but

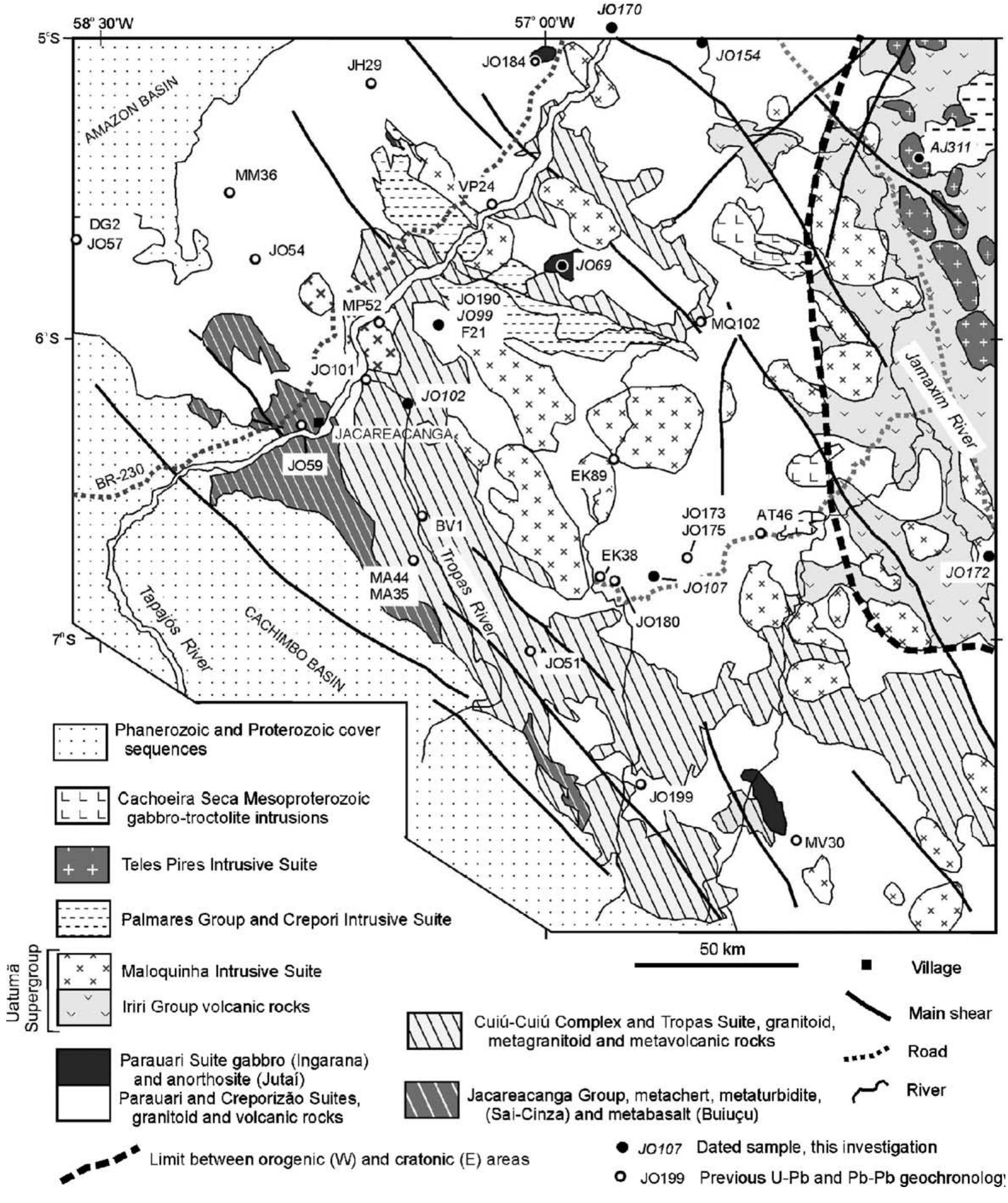


Fig. 2. Geological map of Tapajós Domain with sample location. Based on Faraco et al. (1996).

the field relationships between the two units remain unclear; xenoliths of Jacareacanga Group rocks have not been detected in the Cuiú–Cuiú granitoids.

### 2.2. Cuiú–Cuiú Complex

The first suite of granitoids (Cuiú–Cuiú Complex) consists of large, calc-alkaline tonalite, diorite, quartz-diorite and granodiorite bodies, cut in places by trondhjemite veins and commonly enclosing mafic metavolcanic xenoliths. These are composed mainly of an andesine–hornblende–epidote assemblage, which is diagnostic of amphibolite facies metamorphism. The batholiths are banded and elongated north–northwest parallel to the foliation in the Jacareacanga Group. The mafic xenoliths are either tholeiitic (meta-basalt) or calc-alkalic (meta-andesite) in composition (Almeida et al., 2000).

Pessoa et al. (1977) and Bizzinella et al. (1980) considered the Cuiú–Cuiú rocks to be possibly Archean or Paleoproterozoic. The available Rb–Sr isochron age for this unit is 1800 ± 43 Ma (Tassinari, 1996), much younger than the U–Pb age later determined for the Conceição Tonalite. This tonalite is representative of the Cuiú–Cuiú Complex and was dated at 2011 ± 23 Ma (Santos et al., 1997, 2000), but two of three analyzed zircons are about 10% discordant. Using only the age of grain Z1, which is 100% concordant, the best $^{207}$Pb/$^{206}$Pb age estimate for the rock is 2006 ± 3 Ma. Santos et al. (2001) listed five additional U–Pb ages of Cuiú–Cuiú Complex samples, including sample MQ102 from the type-area of the complex, with the ages falling in the 2040–1998 Ma range, taking into account the uncertainty of each analysis (Table 2).

### 2.3. Creporizão Intrusive Suite

The Creporizão Intrusive Suite was proposed by Ricci et al. (1999) to comprise several monzogranite bodies, which are about 40 million years younger than the Cuiú–Cuiú Complex (J.O.S. Santos, written communication in Ricci et al., 1999). According to these authors, the main characteristic of Creporizão Suite is the presence of protomylonitic texture. Santos et al. (2001) considered the unit mostly late tectonic and composed of calc-alkaline monzogranite and granodiorite plutons (I-type). They dated three samples, including sample JO180 collected at the Creporizão monzogranite type-area, and obtained U–Pb ages in the 1980–1957 Ma range (Table 2). This defined an additional magmatic arc with ages between the older and more primitive Cuiú–Cuiú island arc and the younger Parauari continental arc (Santos et al., 2001). These authors identified preserved volcanic rocks in the Creporizão Arc (sample F21, Fig. 2; 1974 ± 6 Ma) and reported that most rocks related to this arc are undeformed (e.g. sample JO175) lacking protomylonitic texture.

Tassinari (1996) presented a Rb–Sr whole-rock isochron for the Creporizão Village Granodiorite of 1965 ± 16 Ma, which is very similar to ages obtained more recently by zircon U–Pb dating. He provided another Rb–Sr whole-rock isochron for the Creporizão Village Granite of 1732 ± 82 Ma, but this is much younger than the U–Pb ages now available for the same rocks (Santos et al., 2001).

Lamarão et al. (2002) presented the Pb–Pb (evaporation method) ages of 1981 ± 2 Ma and 1983 ± 8 Ma for the “Older” São Jorge Granite and these ages may represent early magmatic activity during the Creporizão Arc evolution.

### 2.4. Parauari Intrusive Suite

The Parauari Intrusive Suite, a granitoid suite that ranges from tonalite to syenogranite, is older than the Maloquinha Intrusive Suite but is intrusive into the Cuiú–Cuiú Complex. The name Parauari is derived from the granitoid which hosts gold mineralization in the Parauari River basin at the Rosa de Maio Mine (Santos et al., 1975). Several authors, including Pessoa et al. (1977), Bizzinella et al. (1980), and Faraco et al. (1996), included all non-foliated or non-banded orogenic granitoids in the Parauari Suite, while the deformed and metamorphosed granitoids were assigned to the Cuiú–Cuiú Complex. However, the available ages for the Parauari granitoids cover a wide range, as follows:

(1) 1951 ± 23 Ma: reference Rb–Sr whole-rock isochron, samples from eight granitoid bodies (Santos and Reis Neto, 1982);
(2) 1965 ± 16 Ma: Rb–Sr whole-rock isochron, Creporizão Granite type-area (Tassinari, 1996);
(3) 1880 ± 12 Ma: conventional zircon U–Pb, Parauari Granite type-area (Santos et al., 1997).

The above ages led Santos et al. (2000) to divide the Parauari Suite into two different suites: Parauari Suite (ages of ca. 1880 Ma) and Creporizão Suite (ages of ca. 1960 Ma). The Parauari Suite, the younger suite as used now, comprises unfoliated, isotropic or porphyritic plutons ranging from gabbro to syenogranite, which are intrusive into both Cuiú–Cuiú and Creporizão granitoids. It is interpreted to be an expanded calc-alkaline plutonic suite (Almeida et al., 1999; Santos et al., 2000; Coutinho et al., 2000).

Zircons from a monzogranite collected in the Parauari Suite type-area (JO54, Fig. 2) provide an upper intercept of 1880 ± 12 Ma from four analysis (Fig. 8 in Santos et al., 2000). However, three of the grains are highly discordant (32, 29 and 27%) and the best estimate for the age of the rock is the $^{207}Pb/^{206}Pb$ age of the single concordant zircon (Z2, 1% discordant), at 1879 ± 2 Ma.

Two samples of Parauari Suite granites (monzogranite EK38 and syenogranite EK89) were dated by zircon Pb–Pb evaporation at the Universidade do Pará isotopic laboratory and the results are published in CPRM survey reports (Klein and Vasquez, 2000; Bahia and Quadros, 2000). The ages are 1883 ± 2 Ma and 1882 ± 4 Ma, respectively.

### 2.5. Post-orogenic assemblage

The post-Tapajós Orogen assemblage consists of four groups of rocks: (1) rocks generated by Uatumã magmatism (Iriri Group and Maloquinha Intrusive Suite); (2) sedimentary cover composed of fluvial deposits; (3) mafic rocks related to several extensional tectonic periods; and (4) rapakivi-like plutonism with uncertain age, but usually considered to be post-Maloquinha (Pessoa et al., 1977; Bizzinella et al., 1980). Rapakivi granites are known far to the southwest in the Rondônia-Juruena Province (Fig. 1) and named the Teles Pires Intrusive Suite of 1762 Ma (Neder et al., 2000).

The orogenic granitoids (Cuiú–Cuiú, Creporizão and Parauari Suites) are cut by rocks generated during Uatumã volcano-plutonic magmatism: a post-orogenic assemblage of evolved orthoclase granites, perthite granites and granophyres (Maloquinha Suite) and calc-alkalic felsic to intermediate pyroclastic and volcanic rocks (Iriri Group). These granitoids are more abundant to the east, towards the boundary with the Central Amazon Province. The previous Rb–Sr whole-rock ages of the Maloquinha Intrusive Suite are 1770 ± 24 Ma (Santos and Reis Neto, 1982) and 1650 ± 20 Ma (Tassinari, 1996). A Rb–Sr whole-rock age from the Iriri Group is 1765 ± 16 Ma (Basei, 1977).

Zircons from an orthoclase granite of the Maloquinha Suite from the Santa Rita Mine (JO199) were dated at 2459 ± 11 Ma (three grains) plus one clearly inherited and concordant grain, dated at 2849 ± 8 Ma (Santos et al., 2000). The age of 2459 Ma is attributed to xenocrystic zircons because it is incompatible with the stratigraphic data, which indicate that the Maloquinha Suite is intrusive into the Parauari granitoids, dated at 1879 Ma. Zircons from four other representative samples of the Maloquinha Suite, including a sample from the type-area in the Tropas River, were dated by SHRIMP U–Pb (Santos et al., 2001) at 1877± 12 Ma, 1874 ± 7 Ma, 1871 ± 8 Ma and 1864 ± 18 Ma. These ages are about 100–220 million years older than the previously determined Rb–Sr ages. A similar SHRIMP U–Pb age of 1870 ± 8 Ma was determined by Santos et al. (2001) for a rhyodacite from the Iriri Group, which is about 210–190 million years older than the Rb–Sr ages of 1680 ± 13 Ma obtained by Basei (1977) and 1650 ± 20 Ma by Tassinari (1996).

Monzogranite batholiths, identified in the lower Jamanxim River basin, were named Santa Helena quartz–monzonite by SUDAM (1972) and Pessoa et al. (1977). Similar rocks were mapped to the south by Bizzinella et al. (1980) and named the Cumaru Intrusive Suite. Both granitoids are Fe-rich, display rapakivi texture, and are dated at 1540 Ma and 1830 Ma, respectively, by Rb–Sr, and have been interpreted as post-orogenic (Pessoa et al., 1977; Bizzinella et al., 1980). The preferred name for this monzogranite suite is Jamanxim rather than Santa Helena, to avoid confusion with the well-known Santa Helena Suite of the southwestern Amazon Craton (Geraldes et al., 2001). There were no previous U–Pb isotopic data to better identify the stratigraphic position of this unit, which is considered to be post-orogenic and younger than the Maloquinha Suite (1.87 Ga).

Younger grabens are filled with fluvial continental sedimentary rocks (Palmares Group) such as quartz sandstone, conglomerate, subarkose, red shale and rare pyroclastic layers, all gently dipping or flat lying. The conglomerates commonly have cobbles and blocks derived from the Maloquinha Suite (Almeida et al., 2000), which establishes a maximum age of about 1870 Ma for their deposition. Gabbroic sills belonging to the tholeiitic Crepori magmatism, cut the Palmares Group and are dated at 1789 ± 9 Ma (SHRIMP U–Pb baddeleyite; Santos et al., 2002). This age indicates that sedimentation occurred between about 1870 and 1790 Ma, providing a correlation with the Roraima Supergroup in northern South America (Santos et al., 2003b).

At least two other mafic units were generated after the end of the Paleoproterozoic: the Cachoeira Seca Troctolite and the Piranhas Dike Swarm. The troctolite, about 1190 Ma old, is related to an extensional far field effect of the Sunsás collision in the western part of the Amazon Craton during the Statherian (Santos et al., 2002). The Piranhas Dike Swarm is related to a Cambrian extensional event (507 Ma), which produced subsidence in the north and instigated deposition of the Amazon Basin sediments (Santos et al., 2002).

## 3. Geochemistry and petrogenesis

Seventy-two samples were analyzed from five of the seven main granitic associations of the Tapajós Domain (Tables DR1, DR2 and DR3) in order to classify chemically the rock-types and to interpret the tectonic environment. The granitic associations are subdivided into seven main groups: Cuiú–Cuiú, Jamanxim, Creporizão, Tropas, Parauari, Maloquinha and Teles Pires granitoids, based on field, petrographic, chemical and geochronological data. The Jamanxim and Teles Pires granitoids were not analyzed because they were only identified near the completion of this work. The Teles Pires ($A_1$-type) and Maloquinha granites ($A_2$-type; Brito et al., 1997) are post-orogenic to anorogenic, but all other five suites are considered to be the product of calc-alkaline arc-related magmatism.

Using the classification diagram of Debon and Le Fort (1983), the granitoids of the Cuiú–Cuiú Complex vary from diorite to granite but are predominantly granodiorites and quartz-monzogabbros (Fig. 3). Only four samples of the Tropas Suite granitoids were analyzed and correspond to quartz-diorites and granites. Modal compositions from thin sections indicate a large amount of tonalites. The Creporizão and Parauari suites show a dominant monzogranitic composition. The Maloquinha Suite plots dominantly in the granite fields, and the Cuiú–Cuiú Complex shows less evolved compositions, including quartz monzogabbro, quartz diorite and granodiorite.

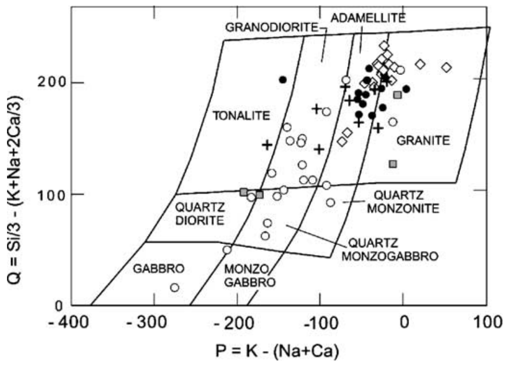


Fig. 3. Multicationic classification diagram (Debon and Le Fort, 1983) showing plutonic associations from the Tapajós Domain. Granitoid symbols: Cuiú–Cuiú: white circle; Creporizão: cross; Tropas: grey square; Parauari: black circle; Maloquinha: white diamond.

The evolutionary trends and degree of maturity of the magmatic arcs of the calc-alkaline and alkaline suites are interpreted on the basis of $SiO_2$, CaO, $Na_2O$ and $K_2O$ contents (Brown, 1982; Brown et al., 1984; Nardi, 1991). The calc-alkaline granitoids from the Tapajós Domain are all within the normal calc-alkaline andesite field, whereas the Maloquinha granites ($A_2$-type) are dominantly metaluminous, alkaline granitoids (Fig. 4).

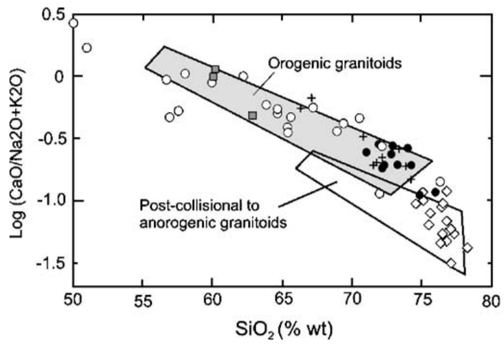


Fig. 4. Plot of $\log(CaO/Na_2O + K_2O)$ vs. $SiO_2$ for granitoids from the Tapajós Domain compared with the range for metaluminous, orogenic, calc-alkaline granitoids (Brown, 1982) and post-collisional to anorogenic granitoids (Nardi, 1991). Symbols as in Fig. 3.

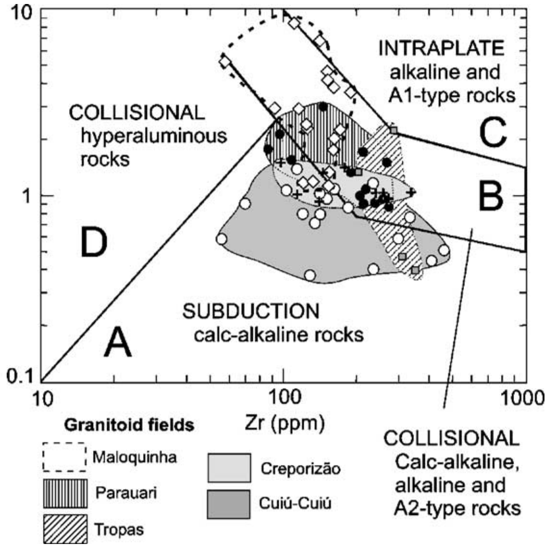


Fig. 5. Geotectonic classification of granitoids from the Tapajós Domain using contents of $(Nb/Zr)_N$ and Zr (Thiéblemont and Tégyey, 1994). Normalization from Hoffman (1988). Symbols as in Fig. 3.

The $(Nb/Zr)_N$ vs. Zr discrimination diagram (Thiéblemont and Tégyey, 1994) also shows similar trends in terms of maturity of arc relationships (Fig. 5). The Cuiú–Cuiú rocks plot preferentially in the field A and have $(Nb/Zr)_N$ ratios > 1, typical of subduction-related magmatic rocks. The Creporizão granitoids plot in the A and B fields, typical of calc-alkaline and alkaline rocks associated with collisional zones, with some similarities to the less-fractionated Cuiú–Cuiú types: $(Nb/Zr)_N$ ratios around 1 and Zr content between 90 and 300 ppm. The Tropas granitoids also plot in the A and B fields, but in contrast with the Creporizão type they have variable $(Nb/Zr)_N$ ratios (0.3–2.0) and some minor variation in Zr content (200–400 ppm). The Parauari granitoid samples fall in the field B (with only a few in the field A) and have moderate to high $(Nb/Zr)_N$ ratios (0.8–2.0). The Maloquinha granites also plot in the field B, with a few samples plotting in the field C (intraplate alkaline rocks), which have the highest $(Nb/Zr)_N$ ratios (1–9) and the lowest Zr contents (50–200 ppm) in comparison with typical within-plate peralkaline granitoids.

Chondrite-normalized whole-rock REE patterns of the Tapajós Domain granitoids are shown in Fig. 6. The Maloquinha granites have a typical A-type "bird wing" pattern. The strong negative Eu anomaly, combined with low Sr, Ba, Ti, P and Zr concentrations, in the Maloquinha granites suggest very strong fractionation of feldspar, Fe–Ti oxides, apatite and zircon. The Creporizão, Tropas and Parauari calc-alkaline granitoids have similar REE patterns; however, the data show that the REE (mostly HREE) become slightly enriched from the Creporizão to the Parauari granitoids. The Cuiú–Cuiú association has broad REE envelopes with two main types. Less fractionated granitoids and diorites are characterized by a discrete negative Eu anomaly and REE contents similar to the Creporizão

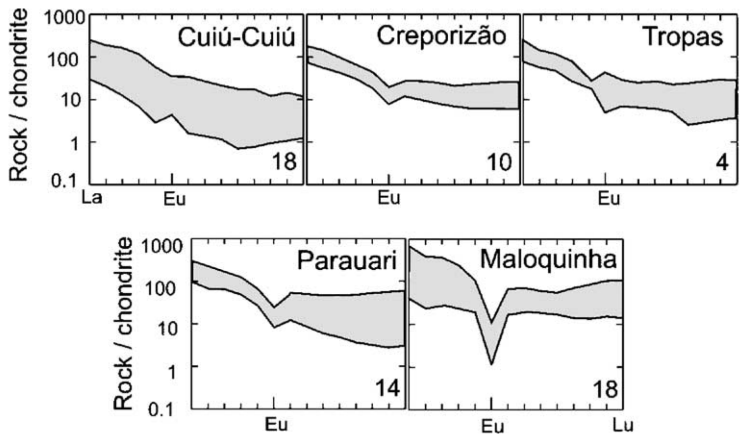


Fig. 6. Chondrite-normalized rare-earth element diagram for the five main granitoid suites from the Tapajós Domain. Grey areas cover the range for each unit. Numbers of samples in lower right corners. Chemical analyses from Table DR3. Normalization from Boynton (1984).

granitoid whereas the highly fractionated granitoids (e.g. $SiO_2 > 70\%$) are represented by highly fractionated REE patterns, low-REE concentrations and a positive Eu anomaly, possibly because of strong hornblende fractionation.

These chemical variations may reflect a decreasing involvement of subducted oceanic lithosphere (Cuiú–Cuiú granitoids) and increasing involvement of the mantle wedge (Creporizão, Tropas and Parauari granitoids) and subcrustal lithosphere (Maloquinha granitoids) during the melting processes and magma generation. In this setting, several processes operated, for examples, partial melting of heterogeneous upper mantle, dehydration and the incorporation into magmas of materials derived from basaltic and sedimentary oceanic crust (Brown et al., 1984). Such crustal material may have been assimilated before fractional crystallization of the magma, a process that seems fundamental for the generation of the igneous suites above subduction zones. However, the complexity of different processes indicated from the trace element variations, makes it difficult to separate the contributions of subduction/crustal-enrichment and within-plate source variations, both active throughout the “maturing” process (Brown et al., 1984). It is probable that subduction-enrichment may occur in the magma source regions of primitive arcs (Cuiú–Cuiú and Tropas rocks) and that crustal contamination may also occur in the more mature arcs (Creporizão and Parauari granitoids). Thus, as these arcs become more mature and magma generation migrates towards regions more remote from the active trench, the influence of the underplating processes becomes larger (Maloquinha granites).

In general, the geochemical trends in granitoids from the Tapajós Province show remarkable consistency, both in their timing and products.

## 4. U–Pb results

Eight samples were investigated by U–Pb geochronology. Table 3 indicates the mineral used (zircon, titanite or baddeleyite), the method (TIMS or SHRIMP) and the laboratory (GSC or UWA). The isotopic results are shown in Tables 4 (SHRIMP) and 5 (TIMS). TIMS data (black ellipses) are combined with SHRIMP data in some plots. All ages presented are $^{207}Pb/^{206}Pb$ ages (average, upper intercept or concordia ages) and all uncertainties are quoted at the $2\sigma$ level. Analytical methods are described in Appendix A.

### *4.1. Jamanxim Monzogranite, JO154, Jamanxim Intrusive Suite*

Sample JO154 is a porphyritic metaluminous hornblende monzogranite to quartz–monzonite collected from the lower Jamanxim River where it is cut by a porphyritic dacite dike. It correlates with the Santa Helena quartz–monzonite of SUDAM (1972) and Pessoa et al. (1977). Due to its rapakivi texture and absence of metamorphism and foliation, and hence has been considered to be related to younger granite

Table 3
Summary of data from samples investigated in this work

| Sample unit | Unit | Latitude (CM=57) | Longitude (CM=57) | Mineral | | | Method | | Laboratory | |
|---|---|---|---|---|---|---|---|---|---|---|
| | | | | z | t | b | TIMS | SHRIMP | GSC | UWA |
| AJ311 | Porquinho Granite | 640340 | 9401125 | x | | | | 1786 ± 14 | | x |
| JO69 | Ingarana Gabbro | 497786 | 9360985 | x | | x | 1887 ± 40 | 1880 ± 2 | x | x |
| JO170 | Uruá Tuff | 578801 | 9496666 | x | | | 1896 ± 40 | 1896 ± 5 | x | x |
| JO99 | Ouro Roxo Tonalite | 457383 | 9319634 | x | x | | 1893 ± 3 | | x | |
| JO172 | São Jorge Monzogranite | 676123 | 9221674 | x | | | | 1907 ± 9 | x | |
| JO102 | Tropas Tonalite | 441214 | 9310873 | x | x | | 1897 ± 2 | | x | |
| JO107 | Joel Monzogranite | 526240 | 9241493 | x | | | 1963 ± 53 | 1968 ± 7 | x | |
| JO154 | Jamaxim Monzogranite | 561948 | 9471224 | x | x | | 1998 ± 6 | 1997 ± 5 | x | |

z: zircon; t: titanite; and b: baddeleyite; CM: central meridian; TIMS: thermal ionization mass spectrometry; SHRIMP: sensitive high-mass resolution ion micro probe; GSC: Geological Survey of Canada; UWA: University of Western Australia.

Table 4
SHRIMP U–Pb data for six samples (ten populations) for samples from the Tapajós Domain of Amazon Craton

| Spot | U (ppm) | Th (ppm) | Th/U | Pb (ppm) | f206[a] (%) | Isotopic ratios[b,c] | | | | Ages[d] | | Conc.[e] (%) |
|---|---|---|---|---|---|---|---|---|---|---|---|---|
| | | | | | | $^{206}Pb/^{238}U$ | $^{207}Pb/^{235}U$ | $^{207}Pb/^{206}Pb$ | $^{208}Pb/^{232}Th$ | $^{206}Pb/^{238}U$ | $^{207}Pb/^{206}Pb$ | |
| Jamaxim Monzogranite, JO154, zircon (GSC) | | | | | | | | | | | | |
| 1-1 | 283 | 224 | 0.82 | 115 | 0.017 | 0.3468 ± 1.51 | 5.9046 ± 1.86 | 0.1235 ± 0.92 | 0.0986 ± 2.08 | 1919 ± 25 | 2007 ± 16 | 96 |
| 2-1 | 412 | 308 | 0.77 | 167 | 0.032 | 0.3514 ± 1.35 | 5.8926 ± 1.86 | 0.1216 ± 1.12 | 0.1006 ± 2.27 | 1941 ± 23 | 1980 ± 20 | 98 |
| 3-1 | 299 | 232 | 0.80 | 122 | 0.053 | 0.3517 ± 1.46 | 5.9571 ± 1.76 | 0.1228 ± 0.82 | 0.1013 ± 2.16 | 1943 ± 24 | 1998 ± 15 | 97 |
| 3-2 | 192 | 152 | 0.81 | 80 | 0.082 | 0.3546 ± 1.32 | 5.9164 ± 1.51 | 0.1210 ± 0.59 | 0.1017 ± 1.47 | 1957 ± 22 | 1971 ± 10 | 99 |
| 2.2 | 168 | 135 | 0.83 | 71 | 0.106 | 0.3630 ± 1.45 | 6.0913 ± 1.80 | 0.1217 ± 0.90 | 0.1026 ± 2.02 | 1997 ± 25 | 1981 ± 16 | 101 |
| 4-1 | 408 | 283 | 0.72 | 166 | 0.026 | 0.3554 ± 1.39 | 5.9863 ± 1.62 | 0.1222 ± 0.67 | 0.1036 ± 1.91 | 1960 ± 24 | 1988 ± 12 | 99 |
| 4-2 | 167 | 127 | 0.78 | 69 | 0.124 | 0.3527 ± 1.37 | 5.8972 ± 1.73 | 0.1213 ± 0.90 | 0.1033 ± 2.21 | 1948 ± 23 | 1975 ± 16 | 99 |
| 4-3 | 179 | 139 | 0.80 | 74 | 0.082 | 0.3568 ± 1.24 | 5.8865 ± 1.72 | 0.1197 ± 1.04 | 0.1021 ± 2.06 | 1967 ± 21 | 1951 ± 19 | 101 |
| 4-4 | 463 | 297 | 0.66 | 181 | 0.055 | 0.3471 ± 1.42 | 5.9044 ± 1.76 | 0.1234 ± 0.88 | 0.0974 ± 1.92 | 1921 ± 24 | 2006 ± 16 | 96 |
| 5-1 | 391 | 227 | 0.60 | 156 | 0.030 | 0.3576 ± 1.26 | 6.0726 ± 1.34 | 0.1232 ± 0.33 | 0.1029 ± 1.88 | 1971 ± 21 | 2003 ± 6 | 98 |
| 5-2 | 416 | 248 | 0.62 | 157 | 0.004 | 0.3368 ± 1.26 | 5.7679 ± 1.93 | 0.1242 ± 1.31 | 0.0978 ± 1.71 | 1871 ± 21 | 2018 ± 23 | 93 |
| 6-1 | 204 | 173 | 0.87 | 84 | 0.036 | 0.3484 ± 1.29 | 5.8211 ± 1.64 | 0.1212 ± 0.86 | 0.1001 ± 2.01 | 1927 ± 22 | 1974 ± 15 | 98 |
| 6-2 | 163 | 125 | 0.79 | 67 | 0.080 | 0.3538 ± 1.35 | 5.9617 ± 2.41 | 0.1222 ± 1.84 | 0.1022 ± 2.04 | 1953 ± 23 | 1989 ± 33 | 98 |
| 7-1 | 371 | 269 | 0.75 | 150 | 0.021 | 0.3524 ± 1.53 | 6.0144 ± 1.80 | 0.1238 ± 0.77 | 0.1003 ± 1.90 | 1946 ± 26 | 2012 ± 14 | 97 |
| 7-2 | 349 | 368 | 1.09 | 155 | 0.046 | 0.3580 ± 1.37 | 6.0463 ± 1.86 | 0.1225 ± 1.10 | 0.1039 ± 1.81 | 1973 ± 23 | 1993 ± 20 | 99 |
| 7-3 | 499 | 431 | 0.89 | 215 | 0.021 | 0.3632 ± 1.29 | 6.1462 ± 1.45 | 0.1227 ± 0.51 | 0.1040 ± 1.80 | 1997 ± 22 | 1996 ± 9 | 100 |
| 7-4 | 366 | 776 | 2.19 | 191 | 0.060 | 0.3462 ± 1.26 | 5.8268 ± 1.64 | 0.1221 ± 0.91 | 0.0987 ± 1.44 | 1916 ± 21 | 1987 ± 16 | 96 |
| 8-1 | 332 | 348 | 1.08 | 145 | 0.090 | 0.3561 ± 1.38 | 5.9923 ± 1.72 | 0.1221 ± 0.86 | 0.1011 ± 1.82 | 1963 ± 23 | 1987 ± 15 | 99 |
| Jamaxim Monzogranite, JO154, titanite (UWA) | | | | | | | | | | | | |
| c.60-1 | 164 | 139 | 0.87 | 51 | 1.123 | 0.3587 ± 1.16 | 6.1603 ± 1.93 | 0.1245 ± 1.54 | 1.2318 ± 1.24 | 1976 ± 20 | 2022 ± 27 | 98 |
| c.62-1 | 122 | 98 | 0.83 | 39 | 1.765 | 0.3690 ± 1.16 | 6.2045 ± 2.33 | 0.1219 ± 2.03 | 1.1824 ± 1.57 | 2025 ± 20 | 1985 ± 36 | 102 |
| c.62-2 | 148 | 121 | 0.84 | 47 | 0.771 | 0.3681 ± 1.17 | 6.2691 ± 1.65 | 0.1235 ± 1.16 | 0.4883 ± 1.43 | 2020 ± 20 | 2008 ± 21 | 101 |
| c.69-1 | 150 | 134 | 0.92 | 46 | 0.435 | 0.3547 ± 1.03 | 6.0277 ± 1.28 | 0.1232 ± 0.76 | 0.0826 ± 1.50 | 1957 ± 17 | 2004 ± 13 | 98 |
| c.70-1 | 116 | 95 | 0.84 | 36 | 0.906 | 0.3612 ± 1.16 | 6.3237 ± 1.95 | 0.1270 ± 1.57 | 0.9427 ± 1.29 | 1988 ± 20 | 2056 ± 28 | 97 |
| c.50-1 | 124 | 105 | 0.87 | 38 | 0.529 | 0.3607 ± 1.04 | 6.1255 ± 1.34 | 0.1232 ± 0.84 | 0.1110 ± 1.45 | 1985 ± 18 | 2003 ± 15 | 99 |
| c.51-1 | 106 | 89 | 0.87 | 34 | 1.848 | 0.3633 ± 1.19 | 5.9675 ± 2.55 | 0.1191 ± 2.25 | 0.8693 ± 1.33 | 1998 ± 20 | 1943 ± 40 | 103 |
| c.63-1 | 178 | 157 | 0.91 | 55 | 0.283 | 0.3590 ± 1.03 | 6.1541 ± 1.23 | 0.1243 ± 0.67 | 0.1615 ± 1.19 | 1977 ± 18 | 2019 ± 12 | 98 |
| c.63-2 | 134 | 111 | 0.86 | 42 | 1.063 | 0.3575 ± 1.12 | 6.0223 ± 1.86 | 0.1222 ± 1.49 | 0.6813 ± 1.63 | 1970 ± 19 | 1988 ± 26 | 99 |
| c.68-1 | 109 | 91 | 0.86 | 35 | 2.735 | 0.3599 ± 1.21 | 5.8870 ± 3.04 | 0.1186 ± 2.79 | 0.9303 ± 1.35 | 1982 ± 21 | 1936 ± 50 | 102 |
| Joel Monzogranite, JO107, zircon (GSC) | | | | | | | | | | | | |
| 2-1 | 139 | 107 | 0.79 | 56 | 0.017 | 0.3483 ± 1.58 | 5.7917 ± 2.29 | 0.1206 ± 1.47 | 0.1015 ± 2.64 | 1927 ± 26 | 1965 ± 26 | 98 |
| 3-1 | 4356 | 1297 | 0.31 | 991 | 0.027 | 0.2235 ± 2.04 | 3.1481 ± 2.84 | 0.1021 ± 1.74 | 0.0592 ± 3.08 | 1301 ± 24 | 1663 ± 33 | 78 |
| 4-1 | 99 | 72 | 0.75 | 40 | 0.017 | 0.3463 ± 1.34 | 5.8094 ± 1.43 | 0.1217 ± 0.35 | 0.1015 ± 3.09 | 1917 ± 22 | 1981 ± 6 | 97 |
| 5-1 | 248 | 166 | 0.69 | 99 | 0.017 | 0.3531 ± 1.25 | 5.9109 ± 1.52 | 0.1214 ± 0.72 | 0.0999 ± 1.90 | 1950 ± 21 | 1977 ± 13 | 99 |
| 6-1 | 82 | 40 | 0.51 | 30 | 0.656 | 0.3418 ± 1.41 | 5.4681 ± 2.12 | 0.1160 ± 1.41 | 0.0912 ± 4.35 | 1896 ± 23 | 1896 ± 26 | 100 |
| 7-1 | 437 | 311 | 0.73 | 177 | 0.008 | 0.3524 ± 1.31 | 5.7897 ± 1.42 | 0.1192 ± 0.40 | 0.1021 ± 1.68 | 1946 ± 22 | 1944 ± 7 | 100 |
| 7-2 | 440 | 258 | 0.61 | 173 | 0.048 | 0.3542 ± 1.32 | 5.8813 ± 1.47 | 0.1204 ± 0.51 | 0.1007 ± 2.01 | 1955 ± 22 | 1963 ± 9 | 100 |
| 7-3 | 235 | 205 | 0.90 | 98 | 0.031 | 0.3507 ± 1.32 | 5.8440 ± 1.48 | 0.1208 ± 0.53 | 0.1028 ± 1.96 | 1938 ± 22 | 1969 ± 10 | 98 |
| 8-1 | 166 | 152 | 0.95 | 63 | 0.067 | 0.3112 ± 1.59 | 5.1681 ± 2.20 | 0.1204 ± 1.34 | 0.1005 ± 1.85 | 1747 ± 24 | 1963 ± 24 | 89 |
| 9-1 | 388 | 284 | 0.76 | 156 | 0.026 | 0.3506 ± 1.28 | 5.8437 ± 1.41 | 0.1209 ± 0.46 | 0.0992 ± 1.44 | 1937 ± 21 | 1970 ± 8 | 98 |
| 10-1 | 160 | 111 | 0.71 | 65 | 0.003 | 0.3526 ± 1.52 | 5.9192 ± 1.91 | 0.1217 ± 0.99 | 0.1041 ± 2.59 | 1947 ± 26 | 1982 ± 18 | 98 |
| 11-1 | 235 | 163 | 0.72 | 94 | 0.017 | 0.3483 ± 1.30 | 5.8828 ± 1.49 | 0.1225 ± 0.58 | 0.0998 ± 1.80 | 1926 ± 22 | 1993 ± 10 | 97 |
| 11-2 | 312 | 160 | 0.53 | 119 | 0.011 | 0.3495 ± 1.27 | 5.7990 ± 1.41 | 0.1204 ± 0.48 | 0.0982 ± 1.71 | 1932 ± 21 | 1962 ± 9 | 99 |
| 13-1 | 207 | 145 | 0.73 | 81 | 0.008 | 0.3416 ± 1.51 | 5.6638 ± 1.78 | 0.1203 ± 0.77 | 0.0965 ± 2.21 | 1894 ± 25 | 1960 ± 14 | 97 |

Table 4 (*Continued*)

| Spot | U (ppm) | Th (ppm) | Th/U | Pb (ppm) | f206[a] (%) | Isotopic ratios[b,c] | | | | Ages[d] | | Conc.[e] (%) |
|---|---|---|---|---|---|---|---|---|---|---|---|---|
| | | | | | | $^{206}Pb/^{238}U$ | $^{207}Pb/^{235}U$ | $^{207}Pb/^{206}Pb$ | $^{208}Pb/^{232}Th$ | $^{206}Pb/^{238}U$ | $^{207}Pb/^{206}Pb$ | |
| São Jorge Monzogranite, JO172, zircon (GSC) | | | | | | | | | | | | |
| 2-1 | 366 | 220 | 0.62 | 140 | 0.017 | 0.3400 ± 1.29 | 5.6439 ± 1.79 | 0.1204 ± 1.10 | 0.1043 ± 2.44 | 1887 ± 21 | 1962 ± 20 | 96 |
| 3-1 | 234 | 139 | 0.61 | 87 | 0.078 | 0.3340 ± 1.23 | 5.3459 ± 1.38 | 0.1161 ± 0.49 | 0.0961 ± 2.12 | 1858 ± 20 | 1897 ± 9 | 98 |
| 4-1 | 220 | 122 | 0.57 | 79 | 0.278 | 0.3267 ± 1.30 | 5.3045 ± 1.74 | 0.1178 ± 0.99 | 0.0945 ± 2.25 | 1823 ± 21 | 1922 ± 18 | 95 |
| 5-1 | 220 | 136 | 0.64 | 82 | 0.728 | 0.3323 ± 1.44 | 5.3249 ± 2.53 | 0.1162 ± 1.91 | 0.0971 ± 3.05 | 1850 ± 23 | 1899 ± 35 | 97 |
| 6-1 | 201 | 118 | 0.61 | 75 | 0.509 | 0.3318 ± 1.50 | 5.3345 ± 2.01 | 0.1166 ± 1.17 | 0.1010 ± 2.10 | 1847 ± 24 | 1905 ± 21 | 97 |
| 6-2 | 176 | 144 | 0.84 | 68 | 0.085 | 0.3307 ± 1.33 | 5.1738 ± 1.83 | 0.1135 ± 1.11 | 0.0964 ± 1.88 | 1842 ± 21 | 1856 ± 20 | 99 |
| 8-1 | 243 | 199 | 0.85 | 97 | 0.080 | 0.3399 ± 1.39 | 5.4888 ± 1.57 | 0.1171 ± 0.59 | 0.0998 ± 1.63 | 1886 ± 23 | 1913 ± 11 | 99 |
| 9-1 | 258 | 151 | 0.60 | 95 | 0.629 | 0.3315 ± 1.70 | 5.3852 ± 2.29 | 0.1178 ± 1.34 | 0.0989 ± 2.18 | 1846 ± 27 | 1923 ± 24 | 96 |
| 10.1 | 113 | 57 | 0.52 | 42 | 0.072 | 0.3386 ± 1.47 | 5.4524 ± 1.91 | 0.1168 ± 1.04 | 0.0989 ± 3.26 | 1880 ± 24 | 1908 ± 19 | 99 |
| 12-1 | 311 | 244 | 0.81 | 134 | 0.017 | 0.3702 ± 1.39 | 6.3248 ± 1.49 | 0.1239 ± 0.38 | 0.1055 ± 1.74 | 2030 ± 24 | 2013 ± 7 | 101 |
| 13-1 | 127 | 50 | 0.40 | 71 | 0.017 | 0.4965 ± 1.35 | 12.9383 ± 1.52 | 0.1890 ± 0.56 | 0.1385 ± 1.98 | 2599 ± 29 | 2733 ± 9 | 95 |
| Uruá felsic tuff, JO170, zircon (GSC) | | | | | | | | | | | | |
| a.1-1 | 146 | 100 | 0.70 | 54 | 0.017 | 0.3260 ± 1.29 | 5.2285 ± 1.62 | 0.1163 ± 0.83 | 0.0917 ± 2.04 | 1819 ± 21 | 1901 ± 15 | 96 |
| a.2-1 | 293 | 226 | 0.80 | 122 | 0.036 | 0.3570 ± 2.10 | 6.1316 ± 2.97 | 0.1246 ± 1.85 | 0.1036 ± 2.79 | 1968 ± 36 | 2023 ± 33 | 97 |
| a.3-1 | 280 | 395 | 1.46 | 125 | 0.006 | 0.3358 ± 1.28 | 5.3704 ± 1.53 | 0.1160 ± 0.69 | 0.0980 ± 1.47 | 1866 ± 21 | 1895 ± 12 | 99 |
| a.3-2 | 142 | 156 | 1.14 | 59 | 0.008 | 0.3310 ± 1.37 | 5.3593 ± 1.92 | 0.1174 ± 1.19 | 0.0966 ± 2.21 | 1843 ± 22 | 1917 ± 21 | 96 |
| a.4-1 | 147 | 185 | 1.30 | 62 | 0.140 | 0.3291 ± 1.26 | 5.2279 ± 1.43 | 0.1152 ± 0.55 | 0.0945 ± 1.58 | 1834 ± 20 | 1883 ± 10 | 97 |
| a.5-1 | 164 | 213 | 1.34 | 76 | 0.019 | 0.3557 ± 1.23 | 6.1114 ± 1.34 | 0.1246 ± 0.39 | 0.1022 ± 2.18 | 1962 ± 21 | 2024 ± 7 | 97 |
| a.6-1 | 251 | 195 | 0.80 | 103 | 0.074 | 0.3510 ± 1.41 | 5.9496 ± 1.66 | 0.1230 ± 0.72 | 0.1003 ± 1.72 | 1939 ± 24 | 1999 ± 13 | 97 |
| a.7-1 | 269 | 280 | 1.08 | 110 | 0.023 | 0.3347 ± 1.29 | 5.3765 ± 1.72 | 0.1165 ± 1.00 | 0.0959 ± 1.70 | 1861 ± 21 | 1903 ± 18 | 98 |
| a.7-2 | 264 | 269 | 1.05 | 111 | 0.071 | 0.3423 ± 1.47 | 5.4457 ± 1.72 | 0.1154 ± 0.74 | 0.1003 ± 1.91 | 1898 ± 24 | 1886 ± 13 | 101 |
| a.9-1 | 287 | 293 | 1.05 | 117 | 0.130 | 0.3347 ± 1.34 | 5.3332 ± 1.64 | 0.1156 ± 0.80 | 0.0964 ± 1.76 | 1861 ± 22 | 1889 ± 14 | 99 |
| a.9-2 | 293 | 319 | 1.12 | 119 | 0.046 | 0.3274 ± 1.62 | 5.3000 ± 1.77 | 0.1174 ± 0.53 | 0.0950 ± 2.27 | 1826 ± 26 | 1917 ± 10 | 95 |
| a.9-3 | 260 | 215 | 0.85 | 99 | 0.064 | 0.3196 ± 1.35 | 5.2156 ± 1.77 | 0.1183 ± 0.99 | 0.0981 ± 2.18 | 1788 ± 21 | 1931 ± 18 | 93 |
| a.9-4 | 157 | 117 | 0.77 | 60 | 0.048 | 0.3312 ± 1.33 | 5.2399 ± 2.72 | 0.1147 ± 2.20 | 0.0964 ± 3.88 | 1844 ± 21 | 1876 ± 40 | 98 |
| a.10-2 | 112 | 102 | 0.94 | 46 | 0.058 | 0.3390 ± 1.81 | 5.4315 ± 2.15 | 0.1162 ± 0.96 | 0.0998 ± 2.63 | 1882 ± 30 | 1899 ± 17 | 99 |
| a.12-1 | 90 | 47 | 0.54 | 34 | 0.102 | 0.3472 ± 1.36 | 5.7184 ± 2.30 | 0.1195 ± 1.69 | 0.1026 ± 2.73 | 1921 ± 23 | 1948 ± 30 | 99 |
| a.13-1 | 221 | 191 | 0.89 | 86 | 0.071 | 0.3276 ± 1.30 | 5.2503 ± 1.50 | 0.1163 ± 0.60 | 0.0954 ± 1.52 | 1826 ± 21 | 1899 ± 11 | 96 |
| a.13-2 | 189 | 123 | 0.67 | 72 | 0.172 | 0.3387 ± 1.31 | 5.3978 ± 1.66 | 0.1156 ± 0.87 | 0.0989 ± 2.03 | 1881 ± 21 | 1889 ± 16 | 100 |
| Uruá felsic tuff, JO170, zircon (UWA) | | | | | | | | | | | | |
| a.61-1 | 46 | 44 | 0.99 | 13 | 0.061 | 0.3384 ± 1.41 | 5.4090 ± 1.77 | 0.1159 ± 1.07 | 0.0944 ± 1.83 | 1886 ± 26 | 1894 ± 19 | 99 |
| a.63-1 | 101 | 98 | 1.00 | 30 | 0.078 | 0.3448 ± 1.48 | 5.4975 ± 1.66 | 0.1156 ± 0.76 | 0.0965 ± 1.69 | 1916 ± 28 | 1890 ± 14 | 101 |
| a.65-1 | 303 | 221 | 0.75 | 83 | 0.126 | 0.3176 ± 0.69 | 5.0983 ± 0.83 | 0.1164 ± 0.45 | 0.0963 ± 1.07 | 1770 ± 12 | 1902 ± 8 | 93 |
| a.66-1 | 306 | 254 | 0.86 | 88 | 0.020 | 0.3361 ± 0.66 | 5.3768 ± 0.79 | 0.1160 ± 0.44 | 0.0954 ± 0.91 | 1870 ± 12 | 1896 ± 8 | 98 |
| a.67-1 | 230 | 210 | 0.94 | 70 | 0.038 | 0.3548 ± 0.73 | 5.6897 ± 0.89 | 0.1163 ± 0.51 | 0.1019 ± 0.92 | 1957 ± 14 | 1900 ± 9 | 103 |
| a.68-1 | 58 | 55 | 0.98 | 17 | 0.152 | 0.3398 ± 1.61 | 5.3853 ± 1.92 | 0.1150 ± 1.05 | 0.0955 ± 2.17 | 1891 ± 30 | 1879 ± 19 | 100 |
| a.69-1 | 221 | 209 | 0.98 | 62 | 0.181 | 0.3279 ± 0.72 | 5.2285 ± 0.95 | 0.1157 ± 0.62 | 0.0951 ± 1.05 | 1827 ± 13 | 1890 ± 11 | 97 |
| a.70-1 | 495 | 358 | 0.75 | 139 | 0.004 | 0.3263 ± 0.59 | 5.2509 ± 0.67 | 0.1167 ± 0.33 | 0.0927 ± 0.71 | 1823 ± 10 | 1907 ± 6 | 95 |
| a.84-1 | 74 | 103 | 1.44 | 23 | 0.022 | 0.3553 ± 1.07 | 5.9982 ± 1.37 | 0.1224 ± 0.86 | 0.1018 ± 1.39 | 1960 ± 22 | 1992 ± 15 | 98 |
| a.88-1 | 58 | 52 | 0.93 | 17 | 0.037 | 0.3333 ± 1.72 | 5.3042 ± 2.02 | 0.1154 ± 1.06 | 0.0968 ± 2.07 | 1853 ± 31 | 1886 ± 19 | 98 |
| a.93-1 | 95 | 98 | 1.08 | 27 | 0.056 | 0.3379 ± 0.80 | 5.4029 ± 1.12 | 0.1160 ± 0.78 | 0.0981 ± 1.15 | 1874 ± 15 | 1895 ± 14 | 99 |
| a.95-1 | 95 | 65 | 0.70 | 28 | 0.067 | 0.3500 ± 0.79 | 5.5779 ± 1.17 | 0.1156 ± 0.86 | 0.1019 ± 1.35 | 1932 ± 15 | 1889 ± 15 | 102 |

| | | | | | | | | | | | | |
|---|---|---|---|---|---|---|---|---|---|---|---|---|
| a.96-1 | 110 | 137 | 1.29 | 31 | 0.165 | 0.3319 ± 0.91 | 5.2434 ± 1.21 | 0.1146 ± 0.79 | 0.0917 ± 1.18 | 1860 ± 18 | 1873 ± 14 | 99 |
| a.99-1 | 117 | 106 | 0.93 | 35 | 0.101 | 0.3453 ± 0.89 | 5.7712 ± 1.13 | 0.1212 ± 0.69 | 0.0950 ± 1.19 | 1921 ± 17 | 1974 ± 12 | 97 |
| a.100-1 | 177 | 129 | 0.75 | 71 | 0.043 | 0.4666 ± 0.75 | 10.3090 ± 0.86 | 0.1602 ± 0.43 | 0.1301 ± 1.11 | 2468 ± 17 | 2458 ± 7 | 100 |
| Ingarana Gabbro, JO69, single zircon (UWA) | | | | | | | | | | | | |
| b.7-2 | 1003 | 1391 | 1.43 | 290 | 0.012 | 0.3363 ± 0.27 | 5.3201 ± 0.36 | 0.1147 ± 0.24 | 0.0967 ± 0.35 | 1869 ± 4 | 1876 ± 4 | 100 |
| b.8-1 | 871 | 411 | 0.49 | 250 | 0.001 | 0.3341 ± 0.25 | 5.2955 ± 0.35 | 0.1149 ± 0.24 | 0.0967 ± 1.18 | 1858 ± 4 | 1879 ± 4 | 99 |
| b.9-1b | 516 | 176 | 0.35 | 148 | 0.016 | 0.3342 ± 0.32 | 5.3189 ± 0.45 | 0.1154 ± 0.32 | 0.0959 ± 1.62 | 1858 ± 5 | 1887 ± 6 | 98 |
| b103-1 | 1809 | 2081 | 1.19 | 536 | 0.003 | 0.3446 ± 0.19 | 5.4603 ± 0.26 | 0.1149 ± 0.18 | 0.0998 ± 0.30 | 1909 ± 3 | 1879 ± 3 | 102 |
| b104-1 | 1636 | 1257 | 0.79 | 476 | 0.005 | 0.3383 ± 0.20 | 5.3511 ± 0.27 | 0.1147 ± 0.18 | 0.0986 ± 0.29 | 1878 ± 3 | 1876 ± 3 | 100 |
| b105-1 | 1836 | 1459 | 0.82 | 535 | 0.000 | 0.3393 ± 0.19 | 5.4096 ± 0.28 | 0.1156 ± 0.21 | 0.0985 ± 0.28 | 1883 ± 3 | 1890 ± 4 | 100 |
| c.7-1 | 891 | 1475 | 1.71 | 255 | 0.022 | 0.3328 ± 0.55 | 5.2735 ± 0.61 | 0.1149 ± 0.26 | 0.0941 ± 0.67 | 1852 ± 9 | 1879 ± 5 | 99 |
| c.8-1 | 1452 | 1632 | 1.16 | 405 | 0.013 | 0.3244 ± 0.29 | 5.1387 ± 0.39 | 0.1149 ± 0.26 | 0.0918 ± 0.48 | 1811 ± 5 | 1878 ± 5 | 96 |
| c.9-1 | 2447 | 3029 | 1.28 | 722 | 0.002 | 0.3432 ± 0.29 | 5.4504 ± 0.33 | 0.1152 ± 0.16 | 0.0960 ± 0.38 | 1902 ± 5 | 1882 ± 3 | 101 |
| c.10-1 | 2797 | 2335 | 0.86 | 807 | 0.001 | 0.3361 ± 0.18 | 5.3300 ± 0.23 | 0.1150 ± 0.14 | 0.0954 ± 0.25 | 1868 ± 3 | 1880 ± 3 | 99 |
| c.10-2 | 2751 | 2149 | 0.81 | 798 | 0.001 | 0.3377 ± 0.20 | 5.3508 ± 0.25 | 0.1149 ± 0.15 | 0.0953 ± 0.26 | 1876 ± 3 | 1879 ± 3 | 100 |
| c.11-1 | 4338 | 6351 | 1.51 | 1358 | 0.002 | 0.3644 ± 0.18 | 5.8091 ± 0.55 | 0.1156 ± 0.52 | 0.1044 ± 0.68 | 2003 ± 3 | 1890 ± 9 | 106 |
| c.14-1 | 1302 | 1361 | 1.08 | 336 | 0.027 | 0.3001 ± 0.24 | 4.7653 ± 0.32 | 0.1151 ± 0.21 | 0.0882 ± 0.83 | 1692 ± 4 | 1882 ± 4 | 90 |
| c.16-1 | 745 | 350 | 0.49 | 228 | 0.478 | 0.3541 ± 0.31 | 6.0286 ± 0.54 | 0.1235 ± 0.45 | 0.0960 ± 1.17 | 1954 ± 5 | 2007 ± 8 | 97 |
| Ingarana Gabbro, JO69, zircon rim aggregate (UWA) | | | | | | | | | | | | |
| b.4-1 | 768 | 549 | 0.74 | 232 | 0.251 | 0.3510 ± 2.18 | 5.6427 ± 2.29 | 0.1166 ± 0.71 | 0.1060 ± 2.25 | 1939 ± 36 | 1905 ± 13 | 102 |
| b.8-1 | 862 | 407 | 0.49 | 245 | 0.001 | 0.3310 ± 0.25 | 5.2454 ± 0.35 | 0.1149 ± 0.24 | 0.0958 ± 1.18 | 1843 ± 4 | 1879 ± 4 | 98 |
| b.9-2 | 511 | 174 | 0.35 | 145 | 0.016 | 0.3310 ± 0.32 | 5.2686 ± 0.45 | 0.1154 ± 0.32 | 0.0950 ± 1.62 | 1843 ± 5 | 1887 ± 6 | 98 |
| b.21-1 | 410 | 270 | 0.68 | 118 | 0.269 | 0.3354 ± 0.37 | 5.2977 ± 0.83 | 0.1146 ± 0.74 | 0.1081 ± 2.64 | 1864 ± 6 | 1873 ± 13 | 100 |
| b.25-1 | 1309 | 823 | 0.65 | 352 | 0.027 | 0.3128 ± 0.26 | 4.9403 ± 0.35 | 0.1145 ± 0.23 | 0.0904 ± 1.86 | 1755 ± 4 | 1873 ± 4 | 94 |
| d.4-1 | 494 | 199 | 0.42 | 160 | 1.192 | 0.3713 ± 0.77 | 5.9619 ± 1.20 | 0.1165 ± 0.91 | 0.2307 ± 3.65 | 2035 ± 14 | 1903 ± 16 | 107 |
| d.5-1 | 430 | 403 | 0.97 | 138 | 1.482 | 0.3684 ± 0.43 | 5.9048 ± 1.47 | 0.1163 ± 1.41 | 0.1041 ± 3.55 | 2022 ± 7 | 1899 ± 25 | 106 |
| d.7-1 | 477 | 278 | 0.60 | 133 | 0.684 | 0.3209 ± 0.40 | 5.0724 ± 0.93 | 0.1146 ± 0.84 | 0.0856 ± 1.69 | 1794 ± 6 | 1874 ± 15 | 96 |
| b.4-1 | 768 | 549 | 0.74 | 232 | 0.251 | 0.3510 ± 2.18 | 5.6427 ± 2.29 | 0.1166 ± 0.71 | 0.1060 ± 2.25 | 1939 ± 36 | 1905 ± 13 | 102 |
| Ingarana Gabbro, JO69, baddeleyite (UWA) | | | | | | | | | | | | |
| b.1-1 | 749 | 31 | 0.04 | 229 | 1.863 | 0.3492 ± 2.34 | 5.4275 ± 3.22 | 0.1127 ± 2.21 | 0.2893 ± 19.6 | 1931 ± 39 | 1844 ± 40 | 105 |
| b.7-1 | 728 | 53 | 0.08 | 248 | 4.620 | 0.3786 ± 2.42 | 5.9739 ± 6.57 | 0.1144 ± 6.11 | 0.5704 ± 17.4 | 2070 ± 43 | 1871 ± 99 | 111 |
| b.14-1 | 1628 | 84 | 0.05 | 515 | 1.266 | 0.3635 ± 2.24 | 5.8826 ± 3.34 | 0.1174 ± 2.48 | 0.3537 ± 10.9 | 1999 ± 38 | 1917 ± 45 | 104 |
| b.18-1 | 2228 | 147 | 0.07 | 722 | 0.188 | 0.3767 ± 2.39 | 5.9533 ± 2.48 | 0.1146 ± 0.64 | 0.1534 ± 7.8 | 2061 ± 42 | 1874 ± 12 | 110 |
| b.18-2 | 762 | 26 | 0.03 | 322 | 1.794 | 0.4831 ± 2.58 | 7.4041 ± 3.77 | 0.1112 ± 2.75 | 0.4030 ± 27.0 | 2541 ± 54 | 1818 ± 50 | 140 |
| b.18-3 | 3303 | 216 | 0.07 | 1068 | 0.034 | 0.3762 ± 2.19 | 5.9563 ± 2.23 | 0.1148 ± 0.39 | 0.1461 ± 2.7 | 2058 ± 39 | 1877 ± 7 | 110 |
| b.31-1a | 529 | 10 | 0.02 | 164 | 0.077 | 0.3609 ± 2.83 | 5.6531 ± 3.09 | 0.1136 ± 1.24 | 0.0656 ± 49.4 | 1986 ± 48 | 1858 ± 22 | 107 |
| b31-1b | 506 | 12 | 0.03 | 139 | 0.191 | 0.3180 ± 2.61 | 5.0747 ± 2.98 | 0.1157 ± 1.43 | 0.0440 ± 49.2 | 1780 ± 41 | 1891 ± 26 | 94 |
| b.31-2a | 1583 | 61 | 0.04 | 491 | 0.311 | 0.3598 ± 2.42 | 5.7477 ± 2.57 | 0.1159 ± 0.86 | 0.2271 ± 7.9 | 1981 ± 41 | 1893 ± 15 | 105 |
| b31-2b | 1698 | 68 | 0.04 | 469 | 0.594 | 0.3198 ± 2.49 | 4.9988 ± 2.83 | 0.1134 ± 1.35 | 0.2136 ± 24.3 | 1789 ± 39 | 1854 ± 24 | 96 |
| b.31-3 | 425 | 9 | 0.02 | 126 | 0.380 | 0.3430 ± 2.44 | 5.4967 ± 2.79 | 0.1162 ± 1.36 | 0.6429 ± 7.1 | 1901 ± 40 | 1899 ± 24 | 100 |
| b.31-4 | 684 | 19 | 0.03 | 197 | 0.150 | 0.3355 ± 2.38 | 5.3462 ± 2.63 | 0.1156 ± 1.12 | 0.1736 ± 15.3 | 1865 ± 39 | 1889 ± 20 | 99 |
| d.3-1 | 1663 | 37 | 0.02 | 516 | 1.396 | 0.3562 ± 2.04 | 5.6607 ± 2.73 | 0.1153 ± 1.81 | 0.1989 ± 34.3 | 1964 ± 35 | 1884 ± 33 | 104 |
| d.3-2 | 1777 | 26 | 0.02 | 586 | 1.251 | 0.3791 ± 0.85 | 6.0488 ± 1.70 | 0.1157 ± 1.47 | 0.3160 ± 34.3 | 2072 ± 15 | 1891 ± 26 | 110 |
| d.3-3 | 1482 | 18 | 0.01 | 505 | 1.024 | 0.3923 ± 1.14 | 6.2568 ± 2.07 | 0.1157 ± 1.74 | 0.5645 ± 25.3 | 2134 ± 21 | 1890 ± 31 | 113 |

Table 4 (*Continued*)

| Spot | U (ppm) | Th (ppm) | Th/U | Pb (ppm) | f206[a] (%) | Isotopic ratios[b,c] | | | | Ages[d] | | Conc.[e] (%) |
|---|---|---|---|---|---|---|---|---|---|---|---|---|
| | | | | | | $^{206}Pb/^{238}U$ | $^{207}Pb/^{235}U$ | $^{207}Pb/^{206}Pb$ | $^{208}Pb/^{232}Th$ | $^{206}Pb/^{238}U$ | $^{207}Pb/^{206}Pb$ | |
| Porquinho Granite, AJ311, zircon (UWA) | | | | | | | | | | | | |
| f.1-1 | 16 | 35 | 2.27 | 4 | 0.066 | 0.3226 ± 1.60 | 4.9105 ± 2.91 | 0.1104 ± 2.43 | 0.0931 ± 2.08 | 1802 ± 25 | 1806 ± 44 | 100 |
| f.3-1 | 46 | 75 | 1.67 | 12 | 0.253 | 0.3144 ± 1.10 | 4.5995 ± 1.49 | 0.1061 ± 1.01 | 0.0918 ± 1.46 | 1762 ± 17 | 1734 ± 18 | 102 |
| f.4-1 | 28 | 32 | 1.21 | 8 | 0.121 | 0.3221 ± 1.29 | 4.8261 ± 1.93 | 0.1087 ± 1.43 | 0.0943 ± 1.79 | 1800 ± 20 | 1777 ± 26 | 101 |
| f.5-1 | 63 | 74 | 1.21 | 17 | 0.097 | 0.3137 ± 1.10 | 4.7638 ± 1.51 | 0.1101 ± 1.04 | 0.0914 ± 1.51 | 1759 ± 17 | 1802 ± 19 | 98 |
| f.6-1 | 28 | 23 | 0.85 | 8 | 0.011 | 0.3266 ± 1.50 | 4.9729 ± 1.88 | 0.1104 ± 1.12 | 0.0940 ± 2.08 | 1822 ± 24 | 1807 ± 20 | 101 |
| f.7-1 | 19 | 39 | 2.05 | 5 | 0.169 | 0.3254 ± 1.44 | 4.9284 ± 2.04 | 0.1099 ± 1.45 | 0.0956 ± 1.91 | 1816 ± 23 | 1797 ± 26 | 101 |
| f.8-1 | 22 | 26 | 1.21 | 6 | 0.429 | 0.3206 ± 1.39 | 4.7325 ± 2.24 | 0.1071 ± 1.76 | 0.0926 ± 1.95 | 1793 ± 22 | 1750 ± 32 | 102 |
| f.9-1 | 15 | 28 | 1.98 | 4 | 0.068 | 0.3199 ± 2.67 | 4.8620 ± 3.39 | 0.1102 ± 2.09 | 0.0933 ± 3.16 | 1789 ± 42 | 1803 ± 38 | 99 |
| f.12-1 | 23 | 29 | 1.29 | 6 | 0.175 | 0.3287 ± 1.57 | 4.8220 ± 2.18 | 0.1064 ± 1.51 | 0.0920 ± 2.21 | 1832 ± 25 | 1738 ± 28 | 105 |
| f.14-1 | 15 | 28 | 1.86 | 4 | 0.246 | 0.3258 ± 1.91 | 4.7561 ± 2.88 | 0.1059 ± 2.15 | 0.0920 ± 2.65 | 1818 ± 30 | 1729 ± 39 | 105 |
| f.15-1 | 21 | 27 | 1.32 | 6 | 0.204 | 0.3245 ± 1.42 | 4.9120 ± 2.14 | 0.1098 ± 1.61 | 0.0932 ± 1.96 | 1812 ± 22 | 1796 ± 29 | 1011 |

*Notes*: GSC: Geological Survey of Canada; UWA: University of Western Australia.

[a] Common $^{206}Pb$/total $^{206}Pb$, based on measured $^{204}Pb$.

[b] All Pb in ratios are radiogenic component. Common lead correction based on $^{204}Pb$ for zircon and titanite and based on $^{208}Pb$ for baddeleyite.

[c] Uncertainties are $1\sigma$, errors in percent.

[d] Ages in Ma, errors are $1\sigma$ absolute.

[e] Concordance: $100t(^{206}Pb/^{238}U)/t(^{207}Pb/^{206}Pb)$.

Table 5
TIMS U–Pb data for six samples (zircon and titanite) from plutons in the Tapajós Domain of Amazon Craton

| Grain | Size[a] (μm) | Weight[b] (μg) | U (ppm) | $^{206}Pb/^{204}Pb$ | Pb[c] (ppm) | $^{206}Pb$[d] (pg) | $^{208}Pb/^{206}Pb$[e] | Isotopic ratios[e,f] | | | $R$[g] | Age[h] | Conc.[i] (%) |
|---|---|---|---|---|---|---|---|---|---|---|---|---|---|
| | | | | | | | | $^{206}Pb/^{238}U$ | $^{207}Pb/^{235}U$ | $^{207}Pb/^{206}Pb$ | | $^{207}Pb/^{206}Pb$ | |
| Jamaxim Monzogranite, JO-154, titanite | | | | | | | | | | | | | |
| TA | 400 | 162 | 116 | 542 | 80 | 782 | 1.14 | 0.3517 ± 0.10 | 5.956 ± 0.25 | 0.12281 ± 0.19 | 0.4150 | 1997 ± 7 | 97 |
| TB | 400 | 301 | 113 | 369 | 88 | 2101 | 1.43 | 0.3533 ± 0.12 | 5.987 ± 0.35 | 0.12291 ± 0.29 | 0.3430 | 1999 ± 10 | 97 |
| Joel Monzogranite, JO-107, zircon | | | | | | | | | | | | | |
| ZA | 100 | 14 | 79 | 10575 | 30 | 2 | 0.19 | 0.3333 ± 0.09 | 5.521 ± 0.10 | 0.12014 ± 0.03 | 0.9549 | 1958 ± 1 | 94 |
| ZB | 150 | 9 | 176 | 11289 | 63 | 3 | 0.13 | 0.3344 ± 0.09 | 5.567 ± 0.10 | 0.12075 ± 0.03 | 0.9545 | 1967 ± 1 | 94 |
| ZC | 150 | 22 | 1698 | 5109 | 463 | 112 | 0.10 | 0.2618 ± 0.08 | 4.030 ± 0.09 | 0.11165 ± 0.03 | 0.9408 | 1826 ± 1 | 80 |
| ZD | 200 | 23 | 2320 | 8921 | 612 | 91 | 0.08 | 0.2569 ± 0.08 | 3.892 ± 0.09 | 0.10990 ± 0.03 | 0.9553 | 1798 ± 1 | 80 |
| Tropas Tonalite, Ouro Roxo gold deposit, JO-99, zircon (ZA, ZB, ZC, ZD, R and S) and titanite ($T_1$, $T_2$ and $T_3$) | | | | | | | | | | | | | |
| ZA | 250 | 22 | 139 | 191 | 55 | 344 | 0.24 | 0.3382 ± 0.19 | 5.476 ± 0.67 | 0.11745 ± 0.56 | 0.6723 | 1918 ± 20 | 98 |
| ZB | 100 | 22 | 90 | 2548 | 35 | 16 | 0.21 | 0.3371 ± 0.08 | 5.382 ± 0.10 | 0.11578 ± 0.05 | 0.9088 | 1892 ± 2 | 99 |
| ZC | 150 | 21 | 307 | 493 | 116 | 254 | 0.21 | 0.3299 ± 1.50 | 5.277 ± 1.90 | 0.11599 ± 1.50 | 0.6276 | 1895 ± 54 | 97 |
| ZD | 200 | 20 | 400 | 6262 | 157 | 24 | 0.27 | 0.3281 ± 0.08 | 5.222 ± 0.10 | 0.11544 ± 0.03 | 0.9486 | 1887 ± 1 | 96 |
| R | 150 | 41 | 243 | 7267 | 93 | 29 | 0.20 | 0.3375 ± 0.08 | 5.402 ± 0.10 | 0.11607 ± 0.03 | 0.8000 | 1897 ± 1 | 99 |
| S | 150 | 31 | 277 | 1966 | 105 | 91 | 0.20 | 0.3339 ± 0.08 | 5.331 ± 0.11 | 0.11578 ± 0.06 | 0.7272 | 1892 ± 2 | 98 |
| $T_1$ | 250 | 203 | 623 | 1456 | 208 | 1699 | 0.03 | 0.3366 ± 0.10 | 5.369 ± 0.14 | 0.11568 ± 0.08 | 0.8389 | 1890 ± 3 | 99 |
| $T_2$ | 200 | 194 | 553 | 1470 | 185 | 1421 | 0.04 | 0.3340 ± 0.09 | 5.324 ± 0.13 | 0.11559 ± 0.08 | 0.8353 | 1889 ± 3 | 98 |
| $T_3$ | 250 | 157 | 357 | 2234 | 119 | 493 | 0.03 | 0.3376 ± 0.09 | 5.381 ± 0.11 | 0.11559 ± 0.05 | 0.8862 | 1889 ± 2 | 99 |
| Tropas Granodiorite, JO-102, zircon ($A_1$, $A_2$, $B_1$ and $B_2$) and titanite ($T_1$, $T_2$ and $T_3$) | | | | | | | | | | | | | |
| $A_1$ | 100 | 12 | 119 | 4581 | 48 | 6 | 0.24 | 0.3400 ± 0.09 | 5.446 ± 0.10 | 0.11617 ± 0.04 | 0.9362 | 1898 ± 1 | 99 |
| $A_2$ | 150 | 11 | 67 | 2576 | 25 | 6 | 0.14 | 0.3419 ± 0.10 | 5.470 ± 0.11 | 0.11603 ± 0.05 | 0.9391 | 1896 ± 2 | 100 |
| $B_1$ | 150 | 8 | 171 | 4324 | 63 | 7 | 0.15 | 0.3390 ± 0.09 | 5.429 ± 0.10 | 0.11615 ± 0.04 | 0.9359 | 1898 ± 1 | 99 |
| $B_2$ | 150 | 14 | 79 | 4486 | 32 | 5 | 0.26 | 0.3411 ± 0.09 | 5.461 ± 0.11 | 0.11611 ± 0.04 | 0.9088 | 1897 ± 1 | 100 |
| $T_1$ | 200 | 177 | 200 | 1503 | 128 | 468 | 1.06 | 0.3398 ± 0.09 | 5.429 ± 0.13 | 0.11588 ± 0.07 | 0.8252 | 1894 ± 3 | 100 |
| $T_2$ | 400 | 333 | 250 | 1524 | 156 | 1081 | 1.01 | 0.3398 ± 0.10 | 5.430 ± 0.13 | 0.11591 ± 0.07 | 0.8456 | 1894 ± 3 | 99 |
| $T_3$ | 300 | 180 | 200 | 1693 | 131 | 429 | 1.07 | 0.3465 ± 0.09 | 5.536 ± 0.12 | 0.11588 ± 0.07 | 0.8545 | 1894 ± 2 | 101 |
| São Jorge Granodiorite, JO-172, zircon (W, X, Y and Z) and titanite(TX and TY) | | | | | | | | | | | | | |
| W | 300 | 33 | 186 | 17101 | 70 | 7 | 0.22 | 0.3271 ± 0.08 | 5.199 ± 0.10 | 0.11526 ± 0.03 | 0.8010 | 1884 ± 1 | 96 |
| X | 150 | 16 | 308 | 1419 | 104 | 63 | 0.24 | 0.2902 ± 0.09 | 4.604 ± 0.13 | 0.11509 ± 0.08 | 0.6920 | 1881 ± 3 | 86 |
| Y | 200 | 14 | 164 | 10587 | 60 | 4 | 0.17 | 0.3268 ± 0.09 | 5.382 ± 0.10 | 0.11941 ± 0.03 | 0.9010 | 1948 ± 1 | 93 |
| Z | 200 | 57 | 304 | 1110 | 96 | 268 | 0.23 | 0.2737 ± 0.09 | 4.293 ± 0.15 | 0.11374 ± 0.10 | 0.6100 | 1860 ± 4 | 82 |
| TX | 400 | 259 | 121 | 140 | 77 | 5353 | 1.01 | 0.3450 ± 0.24 | 5.560 ± 0.94 | 0.11688 ± 0.79 | 0.2560 | 1909 ± 28 | 100 |
| TY | 300 | 187 | 69 | 410 | 55 | 672 | 1.65 | 0.3302 ± 0.11 | 5.271 ± 0.31 | 0.11578 ± 0.25 | 0.3550 | 1892 ± 9 | 97 |
| Uruá Tuff, JO170, zircon | | | | | | | | | | | | | |
| W | 150 | 8 | 74 | 347 | 30 | 37 | 0.23 | 0.3500 ± 0.12 | 5.771 ± 0.35 | 0.11960 ± 0.28 | 0.3420 | 1950 ± 10 | 99 |
| X | 150 | 39 | 188 | 4834 | 67 | 28 | 0.24 | 0.3040 ± 0.08 | 4.792 ± 0.10 | 0.11434 ± 0.04 | 0.8000 | 1870 ± 1 | 90 |
| Y | 100 | 8 | 76 | 3045 | 30 | 4 | 0.31 | 0.3253 ± 0.09 | 5.105 ± 0.11 | 0.11383 ± 0.04 | 0.8180 | 1861 ± 2 | 97 |
| Z | 200 | 34 | 186 | 12721 | 35 | 5 | 0.19 | 0.1695 ± 0.08 | 2.235 ± 0.10 | 0.09563 ± 0.03 | 0.8000 | 1540 ± 1 | 63 |

[a] Sizes in micrometers before abrasion; all fractions are non-magnetic at a side slope of $-0.5^\circ$ on a Frantz isodynamic magnetic separator operating at 1.65 A.
[b] Error on weight is $\pm 1$ mg.
[c] Radiogenic Pb.
[d] Total common Pb on analysis corrected for fractionation and spike.
[e] Corrected for blank Pb and U, common Pb, errors quoted are $1\sigma$ in percent
[f] Measured ratio corrected for spike and Pb fractionation of $0.09 \pm 0.03\%$ per amu.
[g] Correlation of errors in isotope ratios.
[h] Age errors quoted are $2\sigma$ in Ma.
[i] Concordance.

suites, such as the undated Cumaru rapakivi suite of Bizzinella et al. (1980, Chapter 2.5). The zircons in the Jamanxim Monzogranite are fractured and dark, normally with $^{204}$Pb concentrations greater than 100 ppb. An attempt to date these zircons by single-crystal U–Pb TIMS geochronology yielded a discordant result with a $^{207}$Pb/$^{206}$Pb age of 2025 ± 58 Ma. Granitoid JO154 has large titanite crystals (up to 1.2 mm) and these were also dated using TIMS and SHRIMP. Anhedral fragments of reddish-brown titanite, ~500 μm in diameter, were analyzed by SHRIMP. The U content of the titanites is not excessively low (109–178 ppm) and the results are concordant, with the weighted average of 10 analysis resulting in an age of 2008 ± 24 Ma (MSWD = 4.6 (Table 4)). Two grains (TA and TB, Table 5), analyzed by TIMS, are about 3% discordant and have $^{207}$Pb/$^{206}$Pb ages of 1997 ± 7 Ma and 1999 ± 10 Ma. The zircon population was also analyzed by SHRIMP (Table 4) and 17 analyses on 8 grains are concordant to subconcordant, with a weighted mean $^{207}$Pb/$^{206}$Pb age of 1993 ± 6 Ma (MSWD = 1.04) Grain 4 has a younger rim of 1951 ± 19 Ma (spot 4-3, Table 4), which is interpreted as a possible recrystallization associated with Creporizão magmatism, but this assumption it is not definitive considering the large uncertainty of its age. Combining both SHRIMP and TIMS zircon ($n$ = 17) and titanite ($n$ = 12) data in a single concordia plot (Fig. 7) produces the weighed mean $^{207}$Pb/$^{206}$Pb age of 1997 ± 5 Ma (MSWD = 3.70).

The age of 1997 ± 5 Ma for JO154 zircon and titanite is much older than the known age of the typical rapakivi granite suites from the Amazon Craton, formed at 1580–1530 Ma (Bettencourt et al., 1999; Santos et al., 2000). The oldest, previously known, rapakivi granites, located in the Carajás Province, are ca. 1.88 Ga old (Dall'Agnol et al., 1999). The age of JO154 is also older than the ages of all the granitoid suites of the Tapajós Domain, except for the Cuiú–Cuiú Complex. The Jamanxim Monzogranite is older than all rocks from the Creporizão Arc (1980–1957 Ma) and younger than the Cuiú–Cuiú Complex type-area rock (MQ102; 2033 ± 7 Ma), but within error to the younget rock of that complex (MA44 tonalite; 2005 ± 7 Ma). This indicates an intermediate temporal position for the Jamanxim Monzogranite between the Creporizão and Cuiú–Cuiú units. The Cuiú–Cuiú Complex includes most of the rocks formed from 2040 to 1998 Ma (Santos et al., 2001) in the first magmatic arc of the Tapajós–Parima Orogen.

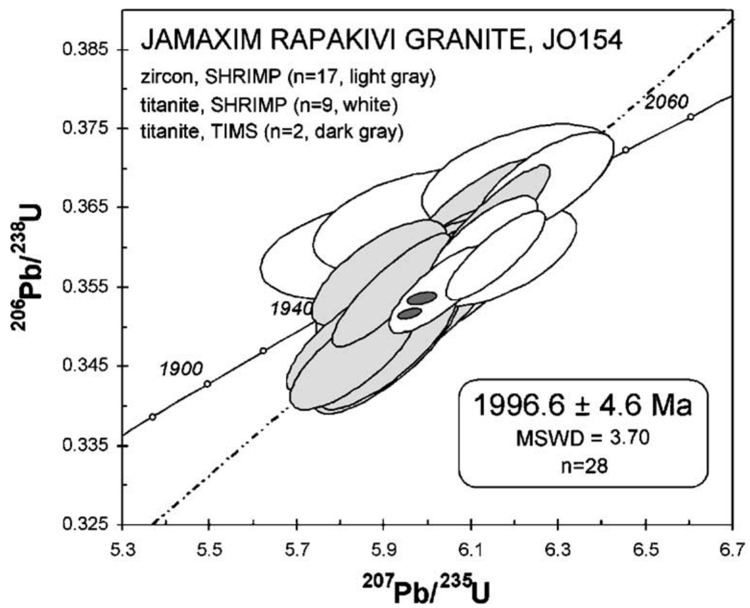


Fig. 7. U–Pb concordia plot of sample JO154, Jamaxim Monzogranite, combining SHRIMP data from zircon (GSC) and titanite (UWA). Uncertainties in this and all others plots are shown at the 2$\sigma$ level.

The age of 1997 ± 5 Ma for JO154 shows that the Jamanxim Monzogranite is much older than previously considered (post-Parauari age is <1880 Ma; Bizzinella et al., 1980) representing a second plutonic magmatic activity in the Tapajós Domain evolution. Similar bodies of rapakivi-textured granitoids (Cumaru Suite) may have similar ages of about 1.99 Ga, possibly representing the oldest known epoch of rapakivi formation in the Amazon Craton. Another example is the Rio Claro batholith, which contains zircon dated at 1997 ± 3 Ma by Pb–Pb evaporation (Vasquez and Klein, 2000).

The presence of late- or post-orogenic and undeformed granitoids in the Cuiú–Cuiú Arc demonstrates that the unit is not composed exclusively of syn-tectonic, deformed rocks, but it includes more evolved and undeformed granitoids. These were intruded during the last stages of the Cuiú–Cuiú Arc development. The previous correlation of the Jamanxim Monzogranite with the rocks of the second continental arc, the Creporizão Suite, is invalid because these are much younger, 1963 ± 6 Ma at the type-area and 1980–1957 Ma overall (Santos et al., 2001).

### *4.2. Joel Monzogranite, JO107, Creporizão Intrusive Suite*

Monzogranite JO107 was collected at the Joel Mine, 12 km to the east of the Creporizão village (Creporizão Suite type-area, Fig. 2). The rock hosts gold mineralization and was correlated with the Parauari Suite (1.88 Ga) in previous investigations (Santos et al., 1997; Klein and Vasquez, 2000). The monzogranite is coarse grained, protomylonitic and altered by hydrothermal fluids to sericite, pyrite, fluorite and adularia. The majority of the zircons are prismatic, aspect ratio 1:1–4:1 and pale yellow, and most of the larger grains (250–400 μm long) are partially metamict. Four grains were analyzed by TIMS, but only the two less discordant (about 6% discordant) data are used on age calculations (Table 5). Twelve SHRIMP analyses on zircon are concordant to sub-concordant (concordance = 97–100%) and two results are discordant (89 and 78%, not used in age calculations, Table 4 and Fig. 8). One grain is younger (1896 Ma) and the main population of 12 concordant or sub-concordant plus 2 TIMS analyses have a weighted mean $^{207}Pb/^{206}Pb$ age of 1968 ± 7 Ma (MSWD = 14;

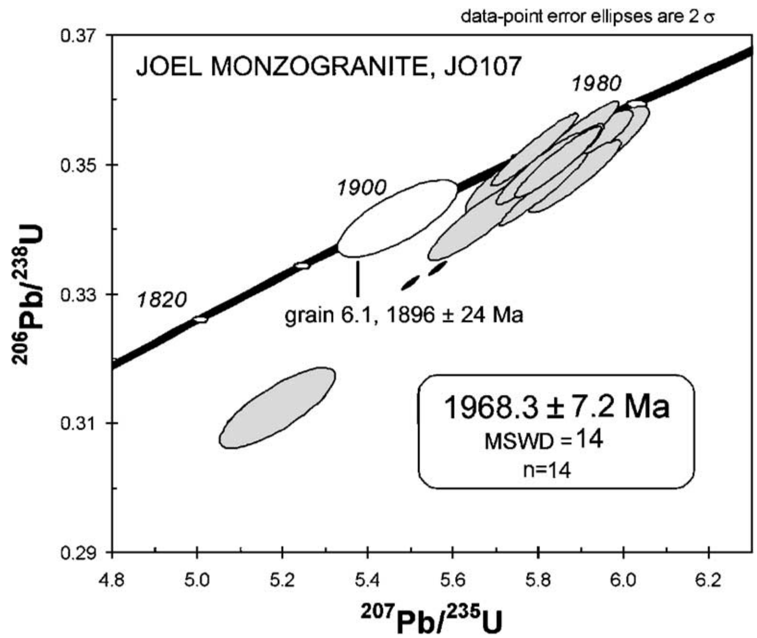


Fig. 8. U–Pb concordia plot of zircon data of sample JO107, Joel Monzogranite. Grey and white ellipses are result of SHRIMP data and the two small black ellipses are product of TIMS data.

Fig. 8) on the concordia plot. The mean average age of this population is 1965 ± 6 Ma (95% confidence; MSWD = 2.4).

Concordant grain 6-1 is distinct because it has the lowest U and Th and highest $^{204}$Pb content among the JO107 zircons. Its age is much younger (1896±24 Ma) than the main population of 1969 ± 8 Ma and it is interpreted to be related to the Tropas Magmatism, perhaps associated with a small granitic vein.

The age of 1968 ± 7 Ma is about 29 million years younger than the Jamanxim Monzogranite age and is within the range of ages of the Creporizão Suite (1980–1957 Ma) determined by Santos et al. (2001). The age of the Joel Monzogranite particularly is similar to that of the JL monzogranite (1966±5 Ma) and to the F21 meta-andesite (1974 ± 6 Ma) dated by Santos et al. (2001; Table 6), and is within error of the age of the Creporizão Monzogranite (1963 ± 6 Ma). The Joel Monzogranite and other rocks associated with the Creporizão Arc are correlated with the Pedra Pintada Suite of the Parima Domain in Roraima (Fig. 1) dated at 1969 ± 4 Ma (Fraga et al., 1997).

### *4.3. Ouro Roxo Tonalite, JO99, Tropas Suite*

This tonalite is the main rock type in the Pacu gold district and has been correlated previously with the Cuiú–Cuiú Complex (Bizzinella et al., 1980; Santos et al., 1997; Almeida et al., 2000), mainly on the basis of degree of deformation and its primitive tonalitic composition. The tonalite has N–S trending banding, which dips to the east, and is affected by several N–S sub-vertical shear zones. It was investigated by the Rio Tinto Zinc and Matapi mining companies, which carried out an exploration program of 28 drill holes. Zircon and titanite were extracted for geochronology from Ouro Roxo Tonalite drill hole 8 (core 168 m) at the Ouro Roxo gold deposit.

The zircon is colourless to light brown with well-defined prismatic shape. The non-magnetic fraction (1.65 A at 0°) was grouped into six fractions (a–d, r and s), which were air abraded and analyzed. The selected titanite grains are light brown to reddish brown anhedral fragments with few or no fractures or inclusions. Titanite was split into three fractions according to colour: clear, dark and intermediate fractions. Six zircon and three titanite grains were analyzed (Table 4). Grains Za and Zc are not used in the age calculation because of their high common lead content (344 and 254 pg) and resulting large errors in isotopic ratios and ages (±54 and ±20 Ma). The results are sub-concordant (99–96%), and the titanite and zircon data yield an upper intercept of 1893 ± 3 Ma (MSWD = 3.2; Fig. 9). Data point *R* is excluded from this regression because it is older (1897 ± 1 Ma) and may represent inherited component.

The age of 1893 ± 3 Ma precludes correlation with the Cuiú–Cuiú Complex (which is about 110 million years older), as well as with the other two regional arc-related units of the Tapajós Domain, namely the Creporizão (1980–1957 Ma) and Parauari (1879 ± 3 Ma) suites. The age of the Ouro Roxo Tonalite is similar to the ages of the Tropas Tonalite (JO102), São Jorge Granodiorite (JO172) and Uruá Felsic Tuff (JO170), and to other samples studied by Santos et al. (2001), such as the Abacaxis Granodiorite (DG2) and Tropas Andesite (JO101). All of these samples have ages in the 1900–1890 Ma interval and represent rocks generated in the fourth arc of the Tapajós Domain, named the Tropas Arc. This arc is composed mainly of tonalite, granodiorite, basalt and andesite, having a geochemistry consistent with an island arc environment (Fig. 5), but also encloses some felsic subaerial volcanic rocks (JO170). Probably most, if not all, tonalites that were related by previous authors (Bizzinella et al., 1980; Klein and Vasquez, 2000; Almeida et al., 2000) to the Parauari Suite are pre-Parauari in age and were formed in the Tropas Arc.

### *4.4. Tropas Tonalite, JO102, Tropas Suite*

The tonalite–basalt–andesite association from the Ouro Roxo gold deposit extends to the south into the lower Tropas River region where sample JO102 was collected (Fig. 2). The rock is a tonalite, displaying the same N–S banding recorded farther north, and contains metabasalt enclaves. These enclaves have an age of 1898 ± 7 Ma (Santos et al., 2001; Table 6) and were originally interpreted as dikes because the tonalite host rock was considered to be related to the Cuiú–Cuiú Complex (Almeida et al., 2000). Tonalite JO102 is zircon rich and the least magnetic fraction at 1.65 A at 0° was split into four abraded fractions ($A_1$, $A_2$, $B_1$, and $B_2$), from which the best grains were picked for analyses. Three titanite grains

Table 6
Summary of new and previous U–Pb ages and sample location for plutono-volcanic rock assemblages of the Tapajós Domain, Amazon Craton

| Reference number | Stratigraphic unit, sample number[1,2,*] | UTM (CM = 57) | | Age (Ma) | Main inheritance ages (Ma) | Reference |
|---|---|---|---|---|---|---|
| | | Easting | Northing | | | |
| Teles Pires Suite–cratonic magmatism | | | | | | |
| 37 | Crepori Dolerite, SD45* | 484503 | 9350059 | 1778 ± 9 ($n$ = 13)[b] | – | 5 |
| **36** | **Porquinho Granite, AJ311*** | 640340 | 9401125 | 1786 ± 14 ($n$ = 11) | – | 1 |
| Uatumã Supergroup: Maloquinha Intrusive Suite and Iriri Group—post-orogenic magmatism | | | | | | |
| 35 | BR230 Granophyre, JO169 | | | 1865 ± 16 ($n$ = 4) | 1998 ± 8 (8) | 3 |
| 34 | Maloquinha Syenogranite, MA35* | 455914 | 9242085 | 1870 ± 4 ($n$ = 15) | 1942 ± 12 (2), 1999 ± 8 (3), 2679 ± 10 (5), 2634 ± 9 (2), 2714 ± 8 | 3 |
| 33 | Pacu Rhyodacite, MM36 | 361575 | 9420057 | 1870 ± 8 ($n$ = 17) | 1955 ± 7 | 3 |
| 32 | Barro Vermelho Granite, BV1 | 452179 | 9281004 | 1873 ± 6 ($n$ = 12) | 1900 ± 18 ($n$ = 4), 2207 ± 8 | 3 |
| 31 | Pepita Syenogranite, MP52 | 429541 | 9335309 | 1872 ± 4 ($n$ = 11) | – | 3 |
| 30 | Santa Rita Granite, JO199 | 538736 | 9165978 | 1874 ± 7 ($n$ = 18) | 1933 ± 10 (2), 1983 ± 19 (3), 2459 ± 11 (3), 2849 (1) | 2 |
| Parauari Intrusive Suite—magmatic arc V | | | | | | |
| 29 | Jutaí Anorthosite, JO184 | 502217 | 9444019 | 1879 ± 8 ($n$ = 25)[t] | – | 3 |
| **28** | **Ingarana Gabbro, JO69 (rims)** | 497786 | 9360985 | 1880 ± 7 ($n$ = 9) | | 1 |
| **27** | **Ingarana Gabbro, JO69** | 497786 | 9360985 | 1881 ± 3 ($n$ = 13) | 2007 ± 6 | 1 |
| 26 | Rosa de Maio Granite, JO54* | 382665 | 9369039 | 1879 ± 3 ($n$ = 1) | – | 2 |
| **25** | **Ingarana Gabbro, JO69** | 497786 | 9360985 | 1881 ± 11 ($n$ = 14)[b] | – | 1 |
| 24 | Post-Crepori Granite, EK89[2] | 528235 | 9301691 | 1882 ± 4 | – | 4 |
| 23 | Crepori Granite, EK38[2] | 517428 | 9246265 | 1883 ± 2 | – | 4 |
| 22 | Penedo Granite, VP24 | 480509 | 9386378 | 1883 ± 4 ($n$ = 15) | – | 3 |
| Tropas Intrusive Suite—magmatic arc IV | | | | | | |
| **21** | **Ouro Roxo Tonalite, JO99** | 457383 | 9319634 | 1893 ± 3 ($n$ = 6)[z+t] | – | 1 |
| 20 | Dacite, RB12[2] | 595198 | 9434928 | 1893 ± 3 | – | 4 |
| 19 | Abacaxis Monzogranite, DG2 | 325416 | 9351136 | 1892 ± 6 ($n$ = 25) | – | 2 |
| **18** | **Tropas Tonalite, JO102[1]*** | 441214 | 9310873 | 1897 ± 2 ($n$ = 7)[z+t] | – | 1 |
| 17 | Tropas Basalt, JO101b | 430631 | 9320811 | 1898 ± 7 ($n$ = 12) | 1972 ± 15 ($n$ = 3) | 2 |
| **16** | **Uruá Tuff, JO170** | 578801 | 9496666 | 1896 ± 5 ($n$ = 23) | 1952 ± 7 ($n$ = 3), 2014 ± 24 ($n$ = 4), 2458 ±7 | 1 |
| **15** | **São Jorge Monzogranite, JO172** | 676123 | 9221674 | 1907 ± 9 ($n$ = 7) | 1962 ± 19; 2013 ± 7; 2733 ± 9 | 1 |
| Creporizão Intrusive Suite—magmatic arc III | | | | | | |
| 14 | Creporizão Monzogranite, JO180* | 480210 | 9246160 | 1963 ± 6 ($n$ = 12) | – | 3 |
| 13 | Km130 Monzogranite, AT46[2] | 564487 | 9250318 | 1968 ± 16 | – | 4 |
| 12 | JL Monzogranite, JO175 | 544782 | 9246153 | 1966 ± 5 ($n$ = 13) | 2003 ± 5 ($n$ = 10) | 3 |
| **11** | **Joel Monzogranite, JO107** | 678131 | 9313311 | 1968 ± 7 ($n$ = 14) | – | 1 |
| 10 | Ouro Roxo Meta-andesite II, F21 | 457710 | 9320150 | 1974 ± 6 ($n$ = 12) | – | 3 |
| Cumaru Intrusive Suite—magmatic arc II | | | | | | |
| 9 | Rio Claro Monzogranite, MV30[2] | | | 1997 ± 3 | – | 4 |
| **8** | **Jamaxim Monzogranite, JO154** | 561948 | 9471224 | 1997 ± 5 ($n$ = 28)[t+z] | – | 1 |
| 7 | Riozinho volcanic rock[2] | | | 1998 ± 3 | – | 6 |

Table 6 (*Continued*)

| Reference number | Stratigraphic unit, sample number[1,2,*] | UTM (CM = 57) | | Age (Ma) | Main inheritance ages (Ma) | Reference |
|---|---|---|---|---|---|---|
| | | Easting | Northing | | | |
| Cuiú–Cuiú Complex—magmatic arc I | | | | | | |
| 6 | Unnamed Tonalite, MA44 | 448730 | 9237714 | 2005 ± 7 (*n* = 13) | – | 3 |
| 5 | Conceição Tonalite, JO51[1] | 481449 | 9201851 | 2006 ± 3 (*n* = 1) | – | 2 |
| 4 | Ouro Roxo Andesite I, JO190 | 457500 | 9320350 | 2012 ± 8 (*n* = 11) | 2040 ± 5 (*n* = 3) | 3 |
| 3 | JL Tonalite, JO173 | 544782 | 9246153 | 2015 ± 9 (*n* = 12) | 2046 ± 5, 2095 ± 15, 2100 ± 7, 2380 ± 8, 2483 ± 19 | 3 |
| 2 | Amana Monzogranite, JH29 | 430115 | 9431055 | 2020 ± 12 (*n* = 5) | – | 3 |
| 1 | Cuiú–Cuiú Tonalite, MQ102* | 512210 | 9362765 | 2033 ± 7 (*n* = 8) | 2056 ± 7 (*n* = 2) | 3 |

Most data are U–Pb SHRIMP, except when indicated in superscript: [1]Conventional U–Pb and [2]Pb–Pb evaporation. Sample from the type-area of each suite is indicated by asterisk after the sample number. Samples dated in this study are in bold face. Most of data on zircon, except when indicated: t: titanite; b: baddeleyite; and z + t: zircon and titanite. Numbers 1–36 are the same of Fig. 3. Sample location on Fig. 2. Number of analyses between brackets (*n* = 10). References 1: this study; 2: Santos et al. (1997), zircon U–Pb TIMS; 3: Santos et al. (2001), U–Pb SHRIMP; 4: Vasquez and Klein (2000), zircon Pb–Pb evaporation; 5: Santos et al. (2002), U–Pb SHRIMP; 6: Lamarão et al. (2002), zircon Pb–Pb evaporation. Numbers 1–37 are the same on Fig. 21.

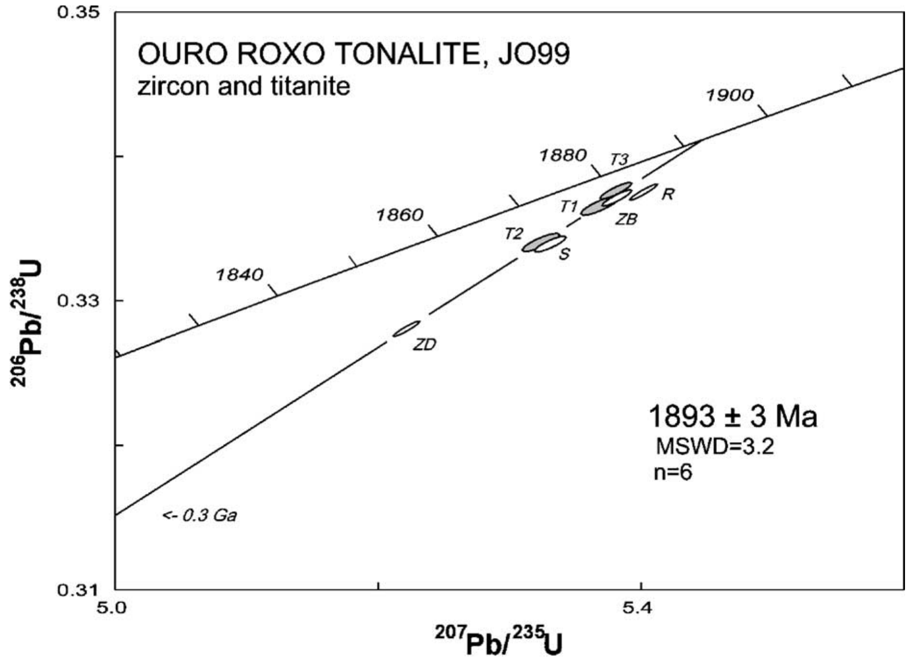


Fig. 9. U–Pb concordia plot of Ouro Roxo Tonalite zircon (S, R, ZB, ZD) and titanite ($T_1$, $T_2$, $T_3$), sample JO99, TIMS data. (GSC).

($T_1$, $T_2$, and $T_3$) were selected, analyzed, and plotted together with the zircon data (Fig. 10). The results are nearly concordant (101–99%; Table 5) and titanites and zircons have the $^{207}Pb/^{206}Pb$ ages of 1897 ± 3 Ma (MSWD = 1.19) and 1894 ± 3 Ma (MSWD = 0.109) (Fig. 10). The mean $^{207}Pb/^{206}Pb$ zircon age is within error (1897 ± 3 Ma) to the mean titanite age (1894 ± 3). The combined age of all seven analysis is 1897 ± 2 Ma (MSWD = 9.6) and this high MSWD may suggest that the titanite is slightly younger than the zircon. These ages demonstrate that the rock is not related to the Cuiú–Cuiú Complex because it is about 105 million years younger, and is slightly older than the Ouro Roxo Tonalite (1893 ± 3 Ma), supporting a correlation with the Tropas Arc. The age of the tonalite is similar to that of the metabasalt enclave (1898 ± 7 Ma; Santos et al., 2001), indicating a short time interval between basaltic volcanism and tonalite intrusion.

### 4.5. *São Jorge Granodiorite, JO172, Tropas Suite*

Sample JO172 is a hornblende granodiorite, main host to gold mineralization at São Jorge. The granodiorite is cut by an orthoclase granite which is similar to the Jardim do Ouro alaskite which crops out about 35 km to the northwest and is dated at 1874 ± 9 Ma (Santos et al., 2001). Sample JO172 comes from the SG2 drill hole, which resulted from a drilling program by Rio Tinto Zinc (Jacobi, 2000). Zircons are colourless and not metamict but highly fractured, generating discordant TIMS results (7–18%), which are not used. Two 300 and 400 μm fragments of clear brown reddish titanite were analyzed by TIMS yielding much more concordant results (Table 5 and Fig. 11). Eleven spot analyses were made on 10 zircon grains on the SHRIMP. Three results (Table 4) represent ages of inherited zircon: one grain (13-1) is Archean (2733 ± 18 Ma); another (12-1) has an age of 2013 ± 14 Ma, possibly derived from the Cuiú–Cuiú Complex; and another (2-1) is 1962 ± 37 Ma old and comparable to the ages of zircon in the Creporizão Arc. The results of the main population ($n = 7$) are concordant and were combined with the two titanite TIMS results and all nine analyses lie on a single discordia regression line having an upper intercept $^{207}Pb/^{206}Pb$ age of 1907 ± 9 Ma (MSWD = 3.5; Fig. 11). This age is within error to the ages of other Tropas Arc rocks, such as JO102 (1897 ± 2 Ma),

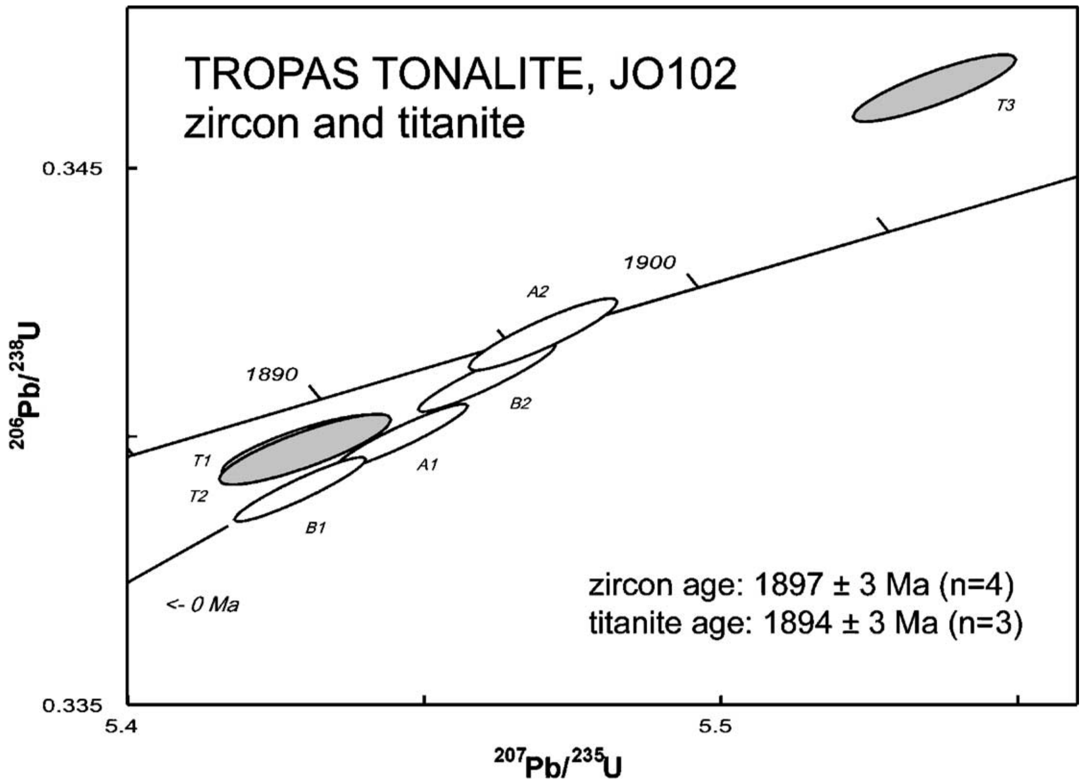


Fig. 10. U–Pb concordia plot of Tropas Tonalite zircon ($A_1$, $A_2$, $B_1$, $B_2$) and titanite ($T_1$, $T_2$, $T_3$), sample JO102, TIMS data (GSC).

JO101 (1898 ± 7 Ma), and JO170 (1897 ± 5 Ma) and indicates that the São Jorge Granodiorite belongs to the Tropas Arc. Grain 6 (1905 ± 21 Ma) has a younger rim of 1856 ± 20 Ma, which is interpreted as local recrystallization related to the apophyses of Jardim do Ouro Granite (1874 ± 9 Ma), which are common in the São Jorge Granodiorite. Lamarão et al. (2002) determined two ages for two different granites at São Jorge region, using Pb–Pb evaporation method. These granites were named Younger São Jorge (1891 ± 3 Ma) and Older São Jorge (1983 ± 8 Ma) granites. These ages are younger and older than the age of sample JO172 and possibly were obtained in different rocks.

Lamarão et al. (2002) determined a Pb–Pb age of 1891 ± 3 Ma for São Jorge Monzogranite (sample F9, named "Younger" São Jorge), another Tropas Arc age, which is slightly younger than the age of sample JO172, and more similar to the age of the Ouro Roxo Tonalite (JO99, 1893 ± 3 Ma).

### 4.6. *Uruá felsic tuff, JO170, Tropas Suite*

The volcanic and pyroclastic rocks covered by the Paleozoic Amazon Basin along the Tapajós River (São Luís and Uruá rapids) have been grouped with the Iriri Group of the Uatumã Supergroup (Ferreira, 1959; Santos et al., 1975). As the Rb–Sr ages of about 1765 Ma from the Iriri Group (Basei, 1977; Tassinari, 1996) are much younger than the zircon U–Pb age of 1870 ± 8 Ma (sample MM36; Santos et al., 2001), another sample was collected for this investigation. Sample JO170 is a felsic tuff collected at the Uruá rapids in the Tapajós River. Four zircon fractions were selected for TIMS (w, x, y, and z) and only one result is nearly concordant (grain w, 1% discordant, Table 5). The age of this grain (w) is ca. 1950 Ma (Table 5) and interpreted to represent an inherited grain comparable in age to the rocks of the Creporizão Arc. The other grains are discordant and were not used in age calculations. In order to obtain

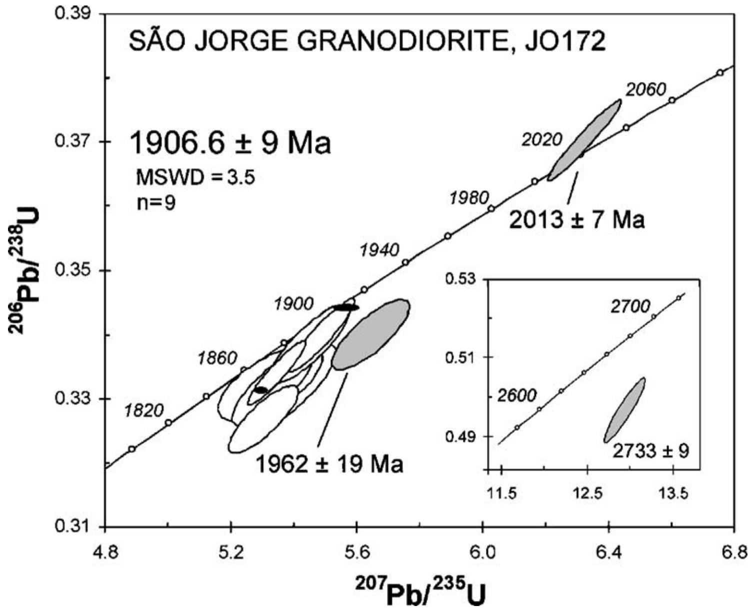


Fig. 11. U–Pb concordia plot of sample JO172, São Jorge Granodiorite (zircon, SHRIMP, GSC) showing magmatic age at $1907 \pm 9$ Ma and inherited ages at $2733 \pm 9$ Ma, $2013 \pm 17$ and $1962 \pm 19$ Ma. Black ellipses are titanite data and shaded ellipses are inherited zircon.

a more reliable age, JO170 zircons were analyzed by SHRIMP both at the GSC (17 analyses) and UWA laboratories (15 analyses) (Table 4). The results of 33 zircon analyses (one TIMS and 32 SHRIMP) on 26 grains indicate four age populations. The oldest zircon (a.100-1) is $2458 \pm 14$ Ma old (Siderian) and the other group (Fig. 12) with weighted averaged $^{207}$Pb/$^{206}$Pb ages of $1896 \pm 5$ Ma ($n = 23$; MSWD = 0.59; $2\sigma$), $1952 \pm 7$ Ma ($n = 3$; MSWD = 0.1; $2\sigma$) and $2014 \pm 23$ Ma ($n = 4$; MSWD = 1.9; $2\sigma$). For grain 9, only analyses 1 and 2 are used; analysis 9-2 (1917 Ma) is not used for age calculations because it is the result of mixed spot covering both core (1932 Ma) and rim (1899 Ma).

The age of the main population ($1896 \pm 5$ Ma) is interpreted to be the crystallization age and supports a correlation of the JO170 tuff to the rocks of the Tropas Arc (Figs. 10 and 11) rather than to the Iriri Group (1870 Ma, Santos et al., 2001), and indicates subaerial felsic magmatism within the Tropas Arc. There is no known source for the inherited age of 2458 Ma, but the other two inherited populations of 2011 and 1970 Ma can be correlated with rocks generated in the Cuiú–Cuiú and Creporizão magmatic arcs.

### *4.7. Ingarana Gabbro, JO69, Parauari Suite*

Sample JO69, collected at the David gold mine, is representative of the Ingarana Gabbro batholith (Pessoa et al., 1977), which is dominated by an augite gabbro facies, but encloses noritic and leucocratic facies. The rock is calc-alkalic, has high $Al_2O_3$ (Bahia and Quadros, 2000), and is zircon-poor: only about 80 grains were recovered from 12 kg of rock. The zircons are brownish prisms, 200–300 μm in length (aspect ratio 1:1–1.5:1), unzoned, U-rich (516–4338 ppm; Tables 4 and 5), Th-rich (350–6351 ppm; Table 5) and highly metamict. Four grains selected for TIMS U–Pb analyses have high $^{204}$Pb contents (about 100 ppb), are 9–20 % discordant, and were discarded. These discordant data define a discordia line intercepting concordia at $1887 \pm 40$ Ma. It was possible with SHRIMP to analyse internal areas of grains, preserved from metamictization (Fig. 13), were analysed by SHRIMP and yielded a more precise $^{207}$Pb/$^{206}$Pb age (Fig. 14) of $1881 \pm 3$ Ma (MSWD = 4.3; $n = 13$). One grain is older and interpreted to be inherited (grain c.16, $2007 \pm 8$ Ma), suggesting crustal contamination of

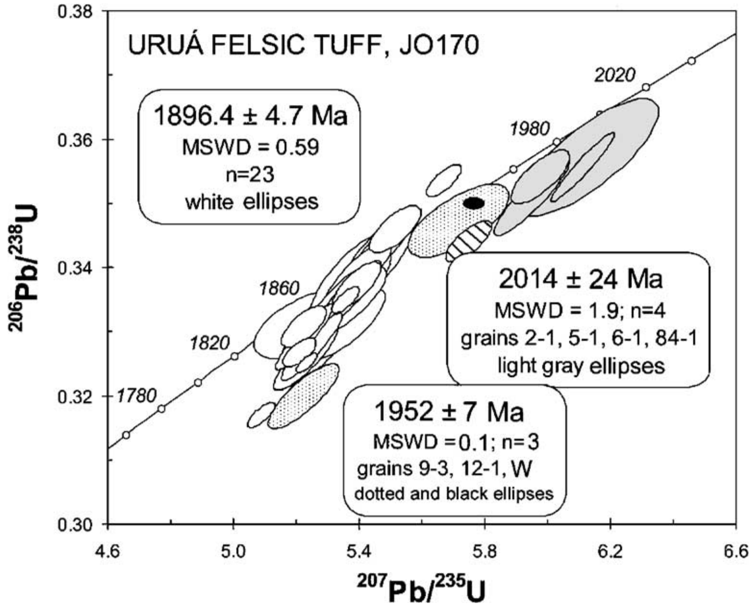


Fig. 12. U–Pb concordia plot of sample JO170, Uruá felsic tuff (zircon, SHRIMP, GSC and UWA), displaying magmatic (1896 ± 5 Ma) and inherited ages of 1952 ± 7 Ma (black and dotted ellipses) and 2014 ± 24 Ma (grey ellipses). Black ellipse represents TIMS data and stripped ellipse is an outlier not used on age calculations.

the gabbroic melt with rocks of the Cuiú–Cuiú Arc. This inherited grain is distinctive from the magmatic population because it is zoned and has an aspect ratio of 3:1. It has lower U (745 ppm) and lower Th/U ratio (0.49) than the magmatic population. A careful search of the heavy mineral concentrate of sample JO69 identified small prisms of baddeleyite. Radiating aggregates of polycrystalline zircon cover all

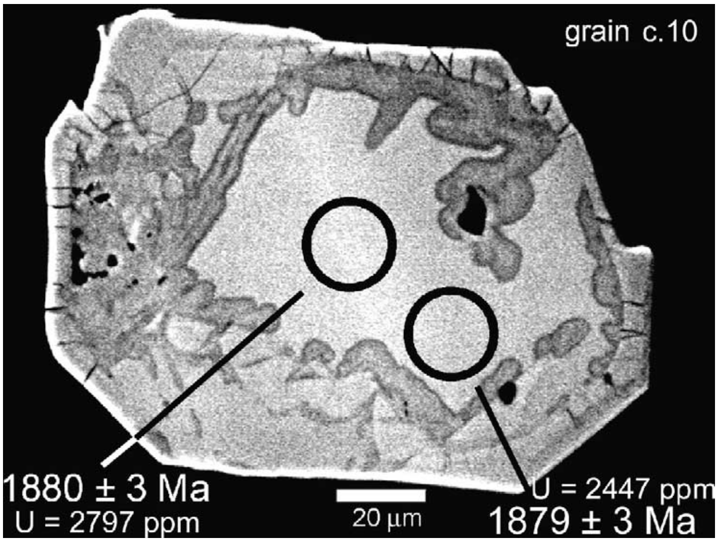


Fig. 13. Back-scattered electrons image of Ingarana Gabbro zircon (grain c.10) showing darker, irregular metamict areas, and clear unaltered, U-rich area where two spot analysis were performed (1880 ± 3 Ma and 1879 ± 3 Ma).

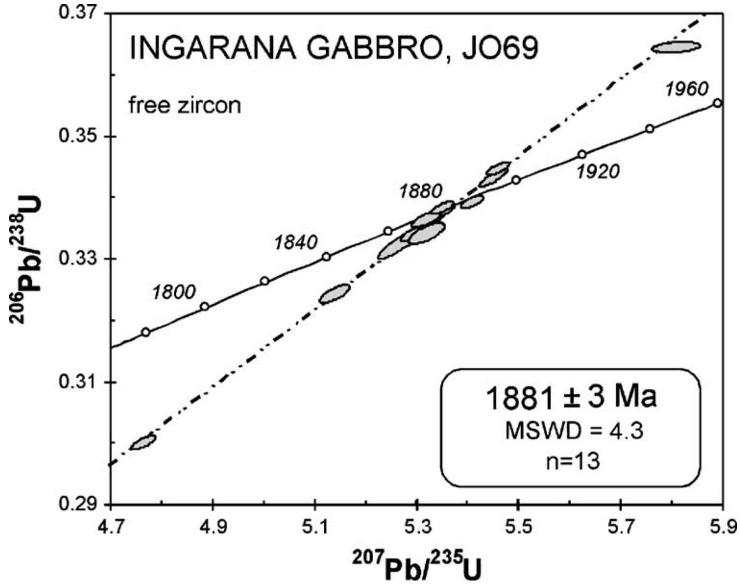


Fig. 14. U–Pb concordia plot of sample JO69, Ingarana Gabbro (zircon, SHRIMP, UWA).

baddeleyite crystals (Fig. 15) and some of these are large enough to be investigated by SHRIMP, along with some baddeleyite cores. Composite crystals are tiny and narrow (10–25 μm wide) and the SHRIMP spot size was reduced to about 10–15 μm to make the analyses possible. The polycrystalline or coronitic (Davidson and Van Breemen, 1988) zircons have lower U, Th and Th/U ratios when compared to the larger, single zircon population. The U–Pb results of the zircon aggregates are less precise (individual

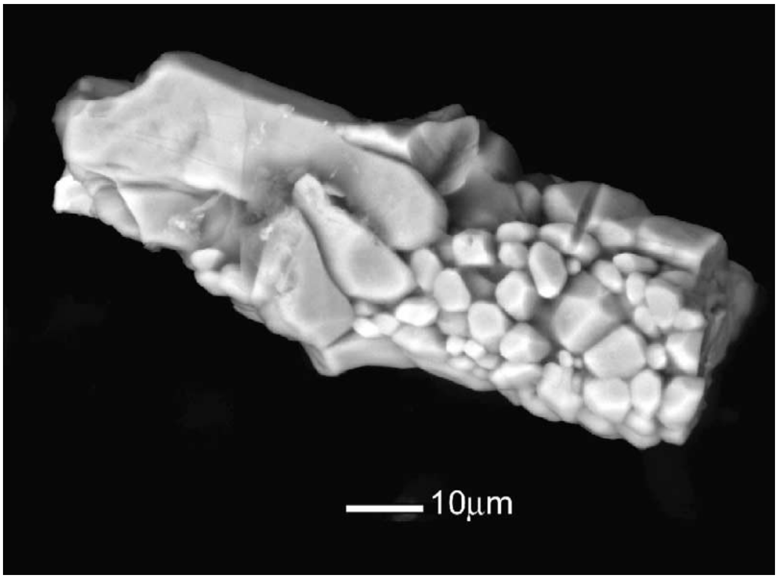


Fig. 15. Back-scattered electrons image of zircon aggregates covering hidden baddeleyite core (JO69). See section on similar composite crystal in Fig. 17.

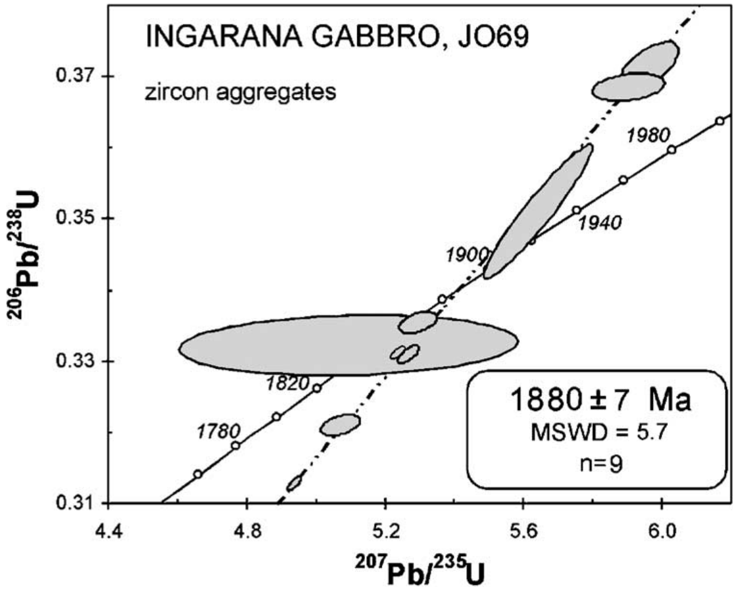


Fig. 16. U–Pb concordia plot of sample JO69, Ingarana Gabbro (zircon rims, SHRIMP, UWA).

$^{207}$Pb/$^{206}$Pb ages errors of 4–25 million years and mean error of 7 million years at 2$\sigma$) in relation to the single zircon grains (individual $^{207}$Pb/$^{206}$Pb ages errors of 3–9 million years and mean error of 2.1 million years at 2$\sigma$) mostly due to the lower U contents and smaller primary ion-beam. This population yields a $^{207}$Pb/$^{206}$Pb age of 1880 ± 7 Ma (MSWD = 5.7; $n = 9$; Fig. 16), which is similar to the age of the zircon single grain population (1881 ± 3 Ma). These ages also match the age of the Parauari Suite

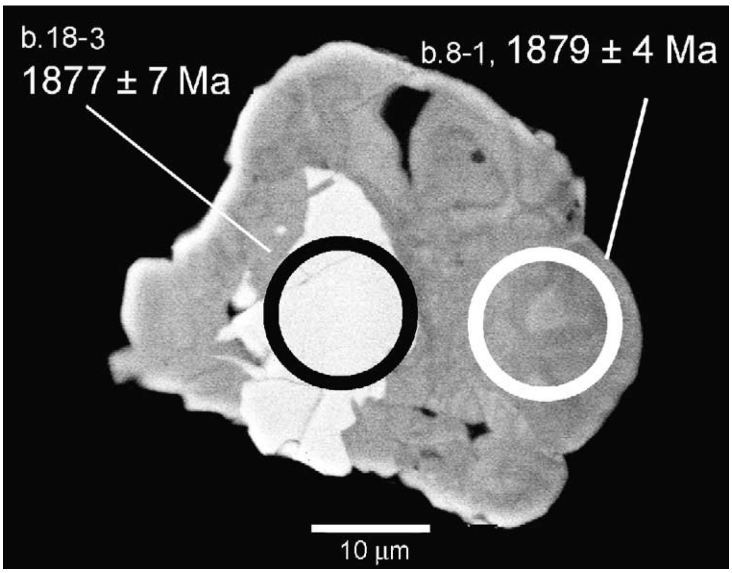


Fig. 17. Back-scattered electrons image of section of composite crystal formed by baddeleyite core (1877 ± 7 Ma) and zircon aggregate rim (1879 ± 4 Ma). Sample JO69.

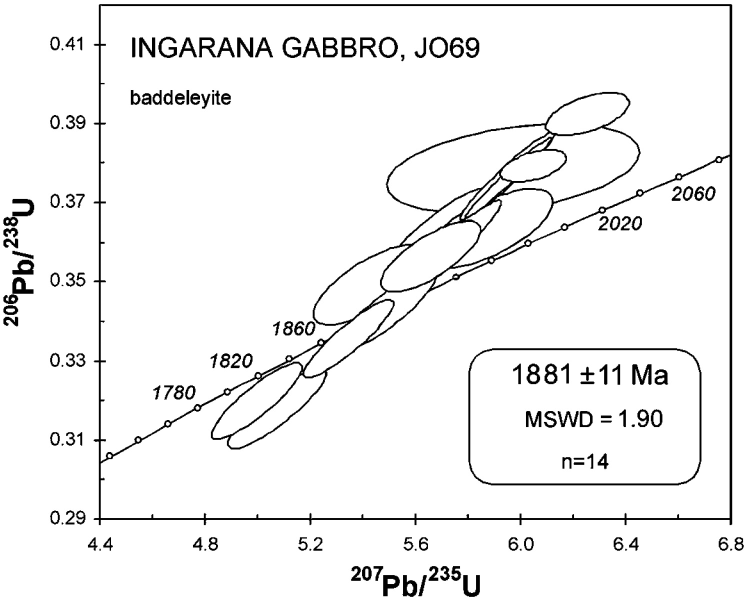


Fig. 18. U–Pb concordia plot of baddeleyite from sample JO69, Ingarana Gabbro (SHRIMP).

granitoids, such as the Rosa de Maio Monzogranite (JO54) at 1879 ± 3 Ma, and the Jutaí anorthosite (1879 ± 8 Ma; $n = 25$; Santos et al., 2001) suggesting the presence of a bimodal suite [gabbro (anorthosite)-granite].

The U–Pb ages of baddeleyite cores (Fig. 17) should represent the age of primary igneous crystallization, whereas the ages of zircon rims should reflect later baddeleyite interaction with silica-rich fluids. The Pb/U results for baddeleyite (Table 4) are

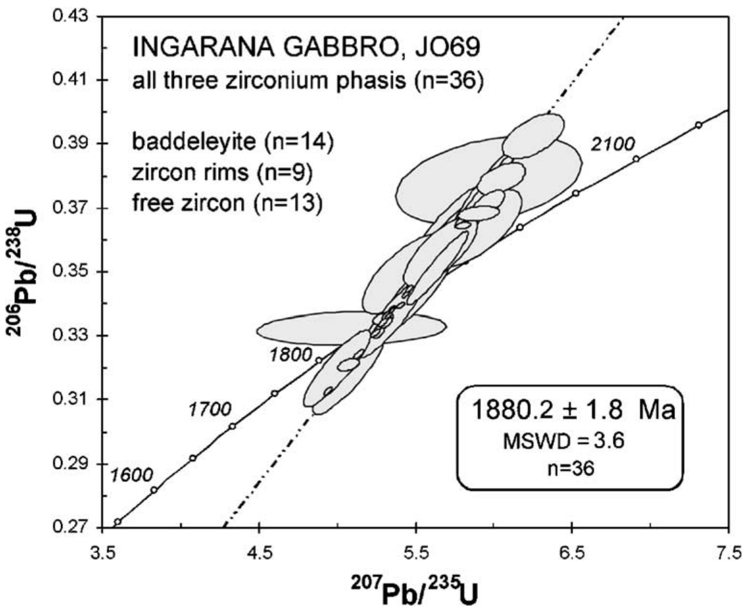


Fig. 19. U–Pb concordia plot of all zirconium-bearing phases of Ingarana Gabbro (JO69).

less precise than those for zircon because: (1) the data are dominantly discordant; and (2) the calibration to the Phalaborwa standard was imprecise because of its low reproducibility. These problems are probably due to crystal orientation effects (Wingate and Compston, 2000). Analysis b.18-2 is 40% discordant and is not used in the calculations. Data for 11 grains are up to 13% reversely discordant. The $^{207}Pb/^{206}Pb$ data are affected by significant common Pb, but give a well-defined weighted mean age (Fig. 18) of $1881 \pm 11$ Ma ($n = 14$; MSWD = 1.9), matching the ages of the two zircon phases.

All three U–Pb ages of Ingarana Gabbro are within error and the combination of all data yields the precise age of $1880 \pm 2$ Ma ($n = 36$; MSWD = 3.60), Fig. 19.

The ages of the Ingarana Gabbro ($1880 \pm 2$ Ma) and Jutaí Anorthosite ($1879 \pm 8$ Ma) date mafic plutonism during evolution of the Parauari Arc (1885–1877 Ma). The Parauari Suite is composed of three main rock-types, monzogranite, syenogranite, and gabbro-anorthosite, and is redefined here as a bimodal suite, instead of an expanded calc-alkalic suite (Santos et al., 1997; Almeida et al., 2000). Most of the tonalites and granodiorites assigned to this unit in the past (Bizzinella et al., 1980) are much older and associated with the Tropas and Cuiú–Cuiú arcs.

### 4.8. Porquinho Granite, AJ311, Teles Pires Suite

Sample AJ311, from the southern facies of the Porquinho Batholith, is an orthoclase granite or alaskite associated with the 1.87 Ga Maloquinha Intrusive Suite (Prazeres et al., 1979; Bahia and Quadros, 2000) and hosts columbite mineralization (Prazeres et al., 1979). Zircon grains are clear, colourless, U-poor (29–122 ppm), with high Th/U ratios (0.85–2.27). Eleven zircon grains were analysed by SHRIMP and the results are mostly concordant (Table 4). The precision of each analysis is relatively poor (18–44 Ma) because of the very low radiogenic Pb content of the grains (4–17 ppm). All 11 analyses groups (Fig. 20) at the age of $1786 \pm 14$ Ma (MSWD of concordance = 1.7; 95% confidence level) when the concordia age of Ludwig (1999) is used. The mean $^{207}Pb/^{206}Pb$ average age at the 95% confidence level is $1778 \pm 16$ Ma (MSWD = 1.5). The zircon population has more Th than U and the $^{208}Pb/^{232}Th$ mean average age, $1779 \pm 20$ Ma (MSWD = 3.20; $2\sigma$), is also reliable. The ages are about 90–100 million years younger than

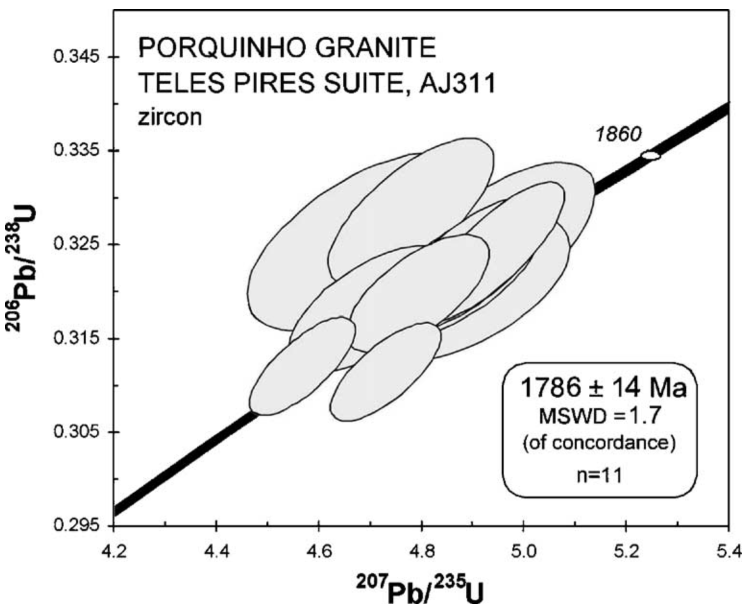


Fig. 20. U–Pb concordia plot of zircon of sample AJ311, Porquinho Granite (SHRIMP).

the age of the Maloquinha Suite (1870 Ma; Santos et al., 2001) providing the first evidence of a second generation of anorogenic granites in the Tapajós Domain. The age of 1786 ± 16 Ma is similar to the age of the Teles Pires Suite in its type-area further south (1793 ± 6 Ma; J.O.S. Santos in Lacerda Filho et al., 2001). This indicates that Teles Pires plutonism is not limited to the south of parallel 8°S or to the south of the Cachimbo Basin (Fig. 1), as proposed by the Amazon Radar Project (Santos et al., 1975; Silva et al., 1980), but extends at least 320 km to the north.

## 5. Integration of new and previous U–Pb data

To better understand the age ranges and evolution of the successive magmatic arcs in the Tapajós Domain, the new U–Pb data are integrated with other isotopic data obtained by TIMS (Santos et al., 1997, 2000), SHRIMP (Santos et al., 2001) and Pb–Pb evaporation techniques (Klein and Vasquez, 2000; Vasquez and Klein, 2000; Lamarão et al., 2002). This integration is shown in Table 6, which includes 37 rock samples dated using zircon, titanite and baddeleyite. The

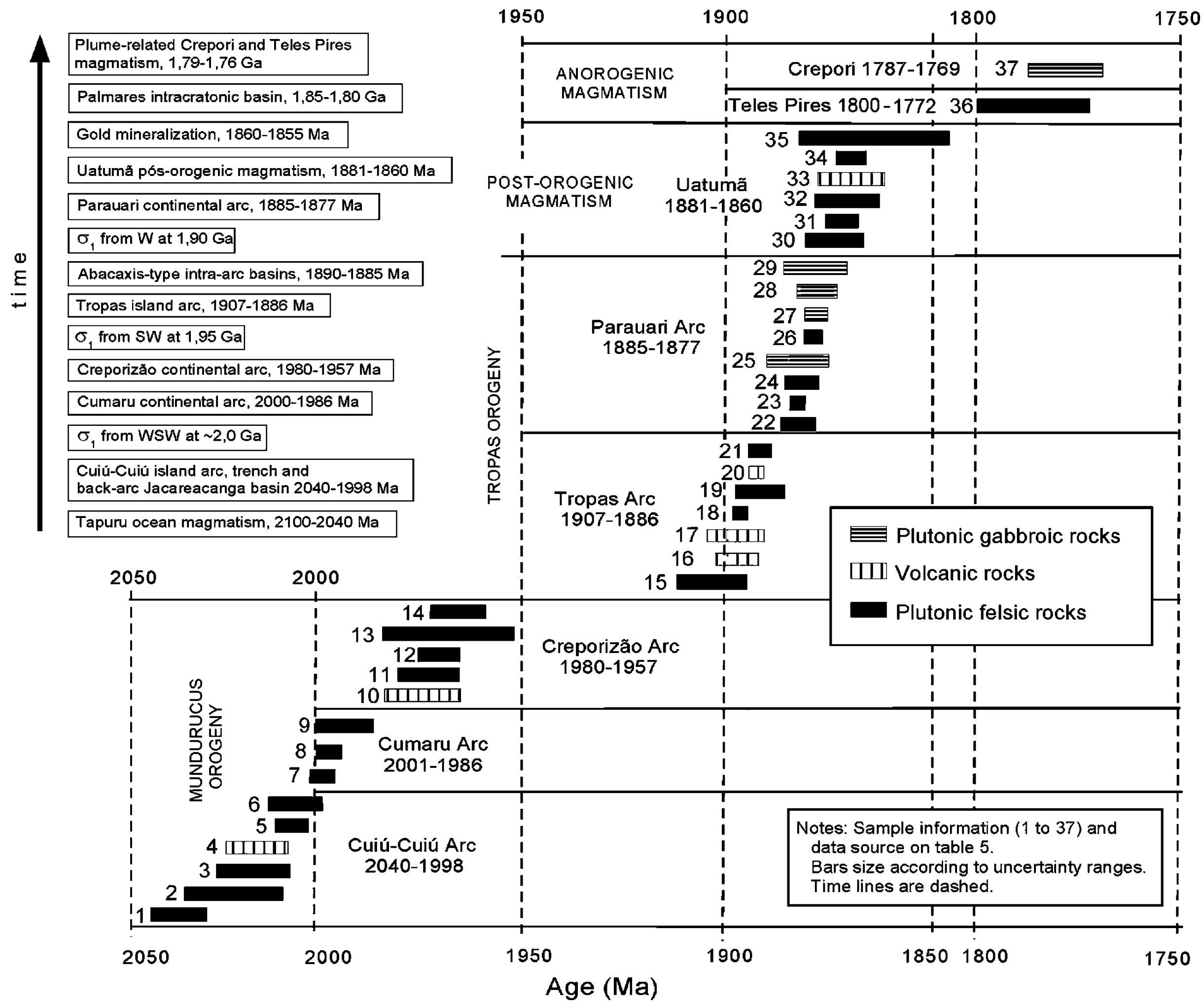


Fig. 21. Temporal distribution of magmatic rocks of the Tapajós Domain, grouped by orogeny and hosting magmatic arc. The upper left hand corner schematically shows the chronological relationship of the magmatic arcs with the sedimentary basins, the main orogenic driving force direction ($\sigma_1$) and gold mineralization. Sample information (1–37) and data source are on Table 6.

Table 7
Ages and possible sources of the inherited zircons detected in rocks of the Tapajós Domain

| Reference number | Sample | Location | Rock | Unit | Magmatic age | Inherited age(s) | Possible source |
|---|---|---|---|---|---|---|---|
| 35 | JO169 | BR230 road | Granophyre | Maloquinha | 1864 ± 19 ($n = 4$) | 1904 ± 19 | Tropas Suite |
| | | | | | | 2000 ± 7 ($n = 9$) | Cuiú–Cuiú Complex |
| 34 | MA35 | Tropas basin | Orthoclase granite | Maloquinha | 1870 ± 4 ($n = 15$) | 1999 ± 8 ($n = 2$) | Cuiú–Cuiú Complex |
| | | | | | | 2634 ± 9 ($n = 2$) | Archean crust |
| | | | | | | 2679 ± 10 ($n = 5$); 2714 ± 8 | Archean crust |
| 33 | MM36 | Pacu River | Rhyodacite | Iriri | 1870 ± 9 ($n = 20$) | 1970 ± 7 ($n = 2$) | Creporizão Suite |
| | | | | | | 1991 ± 11 | Cumaru Suite |
| 30 | JO199 | Santa Rita mine | Syenogranite | Maloquinha | 1874 ± 7 ($n = 18$) | 1983 ± 19 ($n = 3$) | Creporizão Suite |
| | | | | | | 2459 ± 11 ($n = 3$) | Siderian crust |
| | | | | | | 2849 ± 8 | Archean crust |
| 27 | JO69 | David mine | Gabbro | Parauari | 1880 ± 2 ($n = 36$) | 2007 ± 8 | Cuiú–Cuiú Complex |
| 17 | JO101 | Tropas mouth | Metabasalt | Tropas | 1898 ± 7 ($n = 12$) | 1972 ± 15 ($n = 3$) | Creporizão Suite |
| 16 | JO170 | Uruá rapids, Tapajós River | Felsic tuff | Tropas | 1896 ± 5 ($n = 23$) | 1952 ± 7 ($n = 3$) | Creporizão Suite |
| | | | | | | 2014 ± 24 ($n = 4$) | Cuiú–Cuiú Complex |
| | | | | | | 2458 ± 7 | Siderian crust |
| 15 | JO172 | São Jorge gold deposit | Monzogranite | Tropas | 1907 ± 9 ($n = 7$) | 1962 ± 19 | Creporizão Suite |
| | | | | | | 2013 ± 7 | Cuiú–Cuiú Complex |
| | | | | | | 2733 ± 9 | Archean crust |
| 12 | JO175 | JL road | Monzogranite | Creporizão | 1966 ± 5 ($n = 13$) | 2003 ± 5 ($n = 10$) | Cuiú–Cuiú Complex |
| 4 | JO190 | Ouro Roxo gold deposit | Andesite | Cuiú–Cuiú | 2012 ± 8 ($n = 11$) | 2040 ± 5 ($n = 3$) | Tapuru Basalt |
| 3 | JO173 | JL road | Tonalite | Cuiú–Cuiú | 2015 ± 9 ($n = 12$) | 2046 ± 5; 2100 ± 7; 2095 ± 15; | Tapuru Basalt |
| | | | | | | 2380 ± 8; 2483 ± 19 | Siderian crust |
| 1 | MQ102 | Cuiú–Cuiú mine | Tonalite | Cuiú–Cuiú | 2033 ± 7 ($n = 8$) | 2056 ± 7 ($n = 2$) | Tapuru Basalt |

Reference numbers (1–37) are the same of Fig. 21 and Table 6; all ages in Ma.

37 ages are displayed with their uncertainty ranges in Fig. 21. Seven volcano-plutonic units are recognized: five represent orogenic magmatic arcs named Cuiú–Cuiú (I), Jamanxim (II), Creporizão (III), Tropas (IV) and Parauari (V), and two are post-orogenic, named Maloquinha-Iriri and Teles Pires-Crepori.

The upper left hand corner of Fig. 21 schematically shows the chronological relationship of the magmatic arcs with the sedimentary basins, the main orogenic driving force direction ($\sigma_1$) and gold mineralization.

The orogenic granitoids commonly have inherited zircons that are similar in ages to older magmatic suites and are interpreted to be derived from country rocks during either partial melting or contamination. This is most apparent in the monzogranites from the continental arcs, such as Parauari, Creporizão and Jamanxim. Table 7 lists the main inherited ages detected in the Tapajós Domain and their interpretations. Three samples from the Cuiú–Cuiú Complex show inherited zircons with ages of 2095–2040, which, together with ca. 2100 Ma detrital zircons present in the Jacareacanga Group, provides evidence for older magmatic rocks than the Cuiú–Cuiú Complex, possibly positioned to the west of the orogenic belt.

The Creporizão Suite granitoids commonly have inherited zircons, which are correlated to the Cuiú–Cuiú tonalites. Santos et al. (2001) report a population of ten 2003 ± 5 Ma zircons in sample JO175 from the Creporizão Suite (1966 ± 5 Ma), which, integrated with field evidence (Klein and Vasquez, 2000) suggests that the Cuiú–Cuiú tonalites were the source of the Creporizão monzogranitic magma.

The post-orogenic Maloquinha Suite had an important Archean component in the source (samples MA35 and JO199), agreeing with the Sm–Nd model ages of Santos et al. (2000), which suggest derivation from rocks of the Archean Central Amazon Province.

The U–Pb data of the Parauari and Maloquinha suites shown on Table 6 and Fig. 21 may suggest an overlap in their ages, because the difference in these ages is small and because some of used ages have large uncertainties. However, using only the more precise ages (uncertainties of less than 5 million years) the Parauari Suite ages are consistently older than the Maloquinha Suite ages. This is the case comparing the ages of Rosa de Maio Granite (JO54, type-area of Parauari Suite; 1879 ± 3 Ma), Ingarana Gabbro (JO3, 1881 ± 3 Ma), Penedo Granite (VP24, 1883 ± 4 Ma),

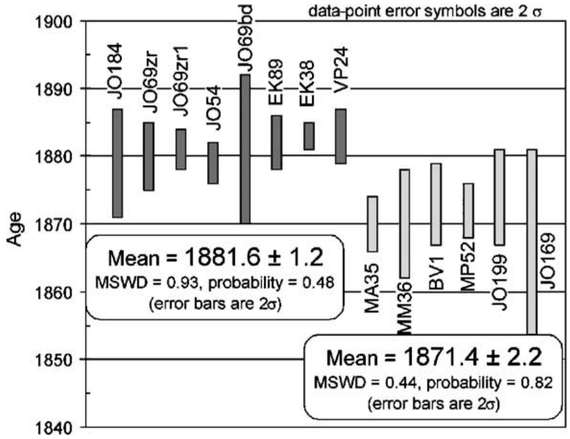


Fig. 22. Weighted averages of Parauari (dark grey bars) and Maloquinha (light grey bars) suites $^{207}Pb/^{206}Pb$ zircon ages forming two distinct clusters at 1881.6 ± 1.2 Ma (Parauari Suite) and 1871.4 ± 2.2 Ma (Maloquinha Suite).

and Crepori Granite (EK38, 1883 ± 2 Ma) to the ages of Maloquinha Granite (MA35, type-area of Maloquinha Suite; 1870 ± 4 Ma), and Pepita Syenogranite (MP52, 1872 ± 4 Ma). There is no overlapping between the Maloquinha and Parauari Suites ages. The $^{207}Pb/^{206}Pb$ ages for both suites using all available data (Table 6) form two distinctive clusters with weighted averages of 1882 ± 1 and 1871 ± 2 Ma (Fig. 22). The conclusion is that the Parauari Suite it is not coeval with the Maloquinha Suite, but slightly older. The difference in their ages may be of about 10 million years, but it is necessary to consider the multiplicity of bodies in both suites and that the temporal relationship between the two units may vary geographically and according to their spatial distribution in relation to the orogenic front.

## 6. Conclusions

In addition to those already defined by Santos et al. (2000), three new magmatic suites are now recognized in the Tapajós Domain: the Jamanxim (a second magmatic arc), Tropas (a fourth magmatic arc) and Teles Pires (a cratonic, rift-related rapakivi granite) suites. The granitic suites are grouped into seven units, five of which are orogenic (Cuiú–Cuiú, Jamanxim, Creporizão, Tropas and Parauari) and two post-orogenic (Maloquinha and Teles Pires). The five early suites have characteristics of calc-alkalic orogenic magmatic arcs and are distinct in age and chemistry from the post-orogenic Maloquinha and Teles Pires suites.

Thus, two groups of Paleoproterozoic rocks, largely granitoids but with subsidiary volcanic and sedimentary components are now clearly recognized in the Tapajós Domain Orosirian rocks formed during the Tapajós–Parima Orogen between 2050 and 1880 Ma, whereas the Orosirian–Statherian post-orogenic and anorogenic assemblages formed between 1870 and 1760 Ma, about 10–120 million years later. The integration of new and previous geochronological data from the south-central region of the Amazon Craton shows that instead of three magmatic arcs (Cuiú–Cuiú, Creporizão and Parauari) which formed during one orogeny, there were five distinctive arcs (Cuiú–Cuiú, Jamanxim, Creporizão, Tropas and Parauari) generated during two main, the Mundurucus and Tropas orogenies separated by about 50 million years (Fig. 21). These constitute the Tapajós–Parima Orogen, which is an Andean-type accretionary orogen in which ocean crust collided with continent crust. The orogen lacks evidence of a continent–continent collisional event. There is no evidence for a continent to the west beyond the oceanic plate, or for the presence of typically collisional rocks, such as S-type granites, paragneisses, granulites and deeply deformed rocks. Both the Mundurucus and Tropas orogenies have a similar evolution starting with a primitive island-arc and finishing with more evolved continental arcs. The similarity of the rocks generated in the temporally distinct epochs makes it difficult to discriminate the units in the field. The Mundurucus orogeny extended from at least 2040 to 1957 Ma, but may pre-date 2040 Ma, if the detrital zircon ages of ca. 2100 Ma from the Jacareacanga Group are associated with magmatism related to primitive rifting of oceanic crust, perhaps represented by the undated Tapuru oceanic basalts.

Associations of folded and metamorphosed tonalite and basalt previously have been related exclusively to the Cuiú–Cuiú Complex, and interpreted to have formed in an island arc environment (Santos et al., 1997, 2000; Bahia and Quadros, 2000; Klein and Vasquez, 2000; Lamarão et al., 2002). However, the current research recognizes a younger island-arc environment with a similar rock association generated during the first stage of the Tropas Orogeny. This rock association constitutes the Tropas Arc (1906–1886 Ma), which is about 100 million years younger than the Cuiú–Cuiú Arc of the Mundurucus Orogeny. Therefore, careful re-evaluation is required of all the geological maps of the region where island arc associations are mapped as the Cuiú–Cuiú Complex (Bizzinella et al., 1980; Almeida et al., 2000; Klein and Vasquez, 2000; Bahia and Quadros, 2000).

The calc-alkalic, metaluminous, high-K monzogranites and syenogranites previously have been assigned to two main arcs, Creporizão and Parauari, but this study defines an older magmatic activity (rapakivi-like post-orogenic magmatism or continental arc?) with similar rocks, the Jamanxim Arc. No petrographic nor geochemical criteria have been developed to discriminate among those three suites and all Jamanxim granitoids have been mapped previously as Parauari or Creporizão suites. This clearly needs re-evaluation.

All felsic to intermediate volcanic rocks in the region previously have been ascribed to a single post-orogenic Uatumã magmatic event which formed the Iriri Group (Santos et al., 1975, 1997; Bizzinella et al., 1980; Bahia and Quadros, 2000). However, this study shows that calc-alkalic volcanic rocks are present not only in the post-orogenic Iriri Group (Santos et al., 2001; sample MM36, 1870 Ma), but in at least four of the orogenic arcs (Cuiú–Cuiú, Creporizão, Tropas, and Parauari): They may be as yet undetected in the poorly known Jamanxim Arc, but their presence requires further investigation. This widespread distribution of calc-alkaline volcanic rocks requires a revision of both the previous concept of Uatumã magmatism and the distribution of rocks proposed to be related to it. Locally, the name Iriri Group should be maintained only for those post-orogenic, calc-alkalic, felsic to intermediate volcanic and pyroclastic rocks associated in time and space with the Maloquinha Intrusive Suite (1870 Ma). Other similar rocks that are orogenic and older should be separately designated.

All evolved, post-orogenic to anorogenic granites previously have been mapped as members of the Maloquinha Suite (Bahia and Quadros, 2000; Klein and Vasquez, 2000; Almeida et al., 2000) emplaced at ca. 1870 Ma. However, recognition of the Porquinho Granite as representative of the ca. 1786 Ma Teles Pires Suite demands revision of previous maps, particularly the Caracol sheet (northeastern part of Fig. 2).

Here, several granite stocks and batholiths are similar to the Porquinho Granite with respect to their circular to elliptical shape and their radiometric (particularly high Th) anomalies.

The youngest orogenic rocks of the Tapajós Domain are about 1880 Ma old (Parauari Suite, Ingarana Gabbro, and Jutaí Anorthosite), precluding correlation of the Tapajós Domain with the Ventuari Domain of Venezuela, as proposed by Tassinari (1996), Tassinari and Macambira (1999) and Tassinari et al. (2000). The oldest orogenic rocks of the Ventuari Domain were formed at 1840–1820 Ma (Macabana and Minicea Gneisses; Gaudette and Olszewski, 1985) during post-Tapajós time and are interpreted as an extension of the Rio Negro Province (Santos et al., 2000) into Venezuela.

The evolution model presented by Lamarão et al. (2002; Fig. 13) is not complete because it was generated by data collected in an area which covers less than 5% of the Tapajós Domain missing several events, such as the Cuiú–Cuiú Arc, Tropas Arc, and Teles Pires cratonic magmatism (Porquinho and Crepori units). That model proposes a subduction-related magmatism during 40 million years (2010–1970 Ma) and identifies the Creporizão continental arc at 1970 Ma, but not recognizing the older Cuiú–Cuiú island arc proposed by Santos et al. (2001), which formation started before 2010 Ma, probably at ca. 2030 Ma according to the age of the Cuiú–Cuiú Complex at its type-area (sample MQ102, 2033 ± 6 Ma; Santos et al., 2001). The age of the Creporizão Suite at its type-area is slightly younger than 1970 Ma (1963 ± 6 Ma; sample JO180 in Santos et al., 2001) and the first orogeny (Mundurucus) forming both Cuiú–Cuiú and Creporizão arcs was developed between ca. 2030 and 1960 Ma having the duration of ∼ 70 million years. Lamarão et al. (2002) envisaged two hypotheses to explain evolution at 1900–1870 Ma, one considering a mature arc evolution (Parauari equivalent) and other proposing a plume activity melting lithospheric mantle. Based on geochronologic (Table 6) and geochemical data (Fig. 4) it is considered that the period of 1910–1880 Ma corresponds to the Tropas Orogeny and that the post-orogenic activity took place only after ca. 1880 Ma, possibly by an underplating process as stated by Santos et al. (2001). Large volume of plutonic and volcanic rocks was generated in a relatively short period of time (ca. 1880–1870 Ma) covering a large area from the eastern Tapajós–Parima Province to the east until the Carajás Province.

The ∼160 million years long orogenic evolution of the Tapajós–Parima Orogen is essentially Orosirian and is roughly coeval with that of the Flin Flon Belt of the Trans-Hudson Orogen (Stern et al., 1995) and the early history of some orogenies of Northeast Laurentia, such as Ungava, Torngat, Rinkian and Ketilidian (Van Kranendonk et al., 1993). Another obvious correlation is with the early Svecofennian Orogen of Baltica (2.0–1.87 Ma; Nironen, 1997). However, while there is an overlap in Baltica between synorogenic and post-orogenic granitoids at 1.880–1.870 Ma (Väisänen et al., 2002) the period 1880–1870 Ma in the Amazon Craton is marked by an absence of orogenic rocks and the formation of hundreds of post-tectonic granite stocks and batholiths (Dall'Agnol et al., 1999).

These correlations with the Trans-Hudson and Svecoffenian orogens suggest that the hypothetical connection of Amazonia with Laurentia and Baltica may have been much older than the Mesoproterozoic as previously suggested (Payolla et al., 2002; Geraldes et al., 2001), perhaps as early as the early Orosirian (2.0 Ga).

## Acknowledgements

Most U–Pb analyses were performed at the Geochronology Laboratory of the Geological Survey of Canada, Ottawa, Canada, with additional U–Pb SHRIMP analyses at the Curtin University of Technology in Perth, Western Australia, which is operated jointly with the University of Western Australia and the Geological Survey of Western Australia with the support of the Australian Research Council. This study is a contribution to the Tapajós Project of the Geological Survey of Brazil and the analytical work was supported financially by the Canadian International Development Agency and the Conselho Nacional de Desenvolvimento Científico e Tecnológico of Brazil. We thank to Vicki McNicoll from the Geological Survey of Canada for a detailed revision. Reviewer suggestions (Prof. Marcio Pimentel) improved considerably this manuscript. We are grateful to Dr. Yvon Maurice, Geological Survey of Canada, for his strong incentive to investigate the Tapajós region.

## Appendix A

### A.1. Sampling and analytical procedures

Location of sampling sites for geochronology is shown in Fig. 2 whereas Table 3 displays information about mineral petrography (zircon, titanite or baddeleyite), techniques (TIMS and SHRIMP) and laboratories used (GSC or UWA). Seven samples weighing about 2–3 kg were collected from each site, except for gabbro sample JO69 which was about 12 kg. The U–Pb isotopic data reported here were measured in 1998 and 2000 at the Geological Survey of Canada Geochronology Laboratory (samples JO69, JO99, JO102, JO107, JO154, JO170, JO172, JO174), and in 1998 and 1999 at the University of Western Australia (samples JO69, AJ311, and JO170). Analyses were obtained by conventional thermal ionization mass spectrometry at the GSC Laboratory and by SHRIMP II (sensitive high-mass resolution ion micro probe) at both the GSC and UWA laboratories. Samples were crushed, milled and sieved at 60 mesh and the heavy minerals were separated using heavy liquid and magnetic separation techniques. The final separation of the minerals was by hand picking the suitable minerals and rejecting the more fractured, metamict and inclusion-rich grains. Samples JO102 and JO99 have some colourless, transparent, crack-free, and inclusion-free zircon, while samples JO69 and JO154 have only coloured and fractured zircon. Samples with highest quality zircon were selected for TIMS analyses, and the others for SHRIMP analyses.

For TIMS analyses, all zircon fractions were strongly abraded until the crystals assumed a well rounded shape (Krogh, 1982); Analytical techniques for measuring U–Pb isotopes in zircon at the Geological Survey of Canada are summarized in Parrish et al. (1987), and are based on Krogh (1973). Mass spectrometry, data reduction, and method of propagation of analytical uncertainties of the relevant components in the calculation of isotopic ratios and ages followed the numerical procedure of Roddick et al. (1987).

Zircon samples for TIMS were hand picked from the least magnetic fraction (non-magnetic at 1.65 A at 0°), and were strongly air-abraded using a technique similar to that described by Krogh (1982). This was done to minimize the effects of peripheral lead loss and/or to remove metamorphic rims. Suitable single zircon crystals were then chosen from the abraded fractions, spiked with a mixed $^{205}$Pb–$^{233}$U–$^{235}$U tracer (Parrish and Krogh, 1987), and dissolved in Teflon micro-capsules. Analytical techniques for measuring U–Pb isotopes in zircon at the Geological Survey of Canada are summarized in Parrish et al. (1987), and are based on Krogh (1973). Mass spectrometry, data reduction, and method of propagation of analytical uncertainties of the relevant components in the calculation of isotopic ratios and ages followed the numerical procedure of Roddick et al. (1987). Initial common lead composition was estimated using the Stacey and Kramers (1975) growth curve. The decay constants used are those recommended by IUGS (Steiger and Jäger, 1977). A modified form of York's (1969) method for linear regression analysis was used (see Parrish et al., 1987). TIMS isotopic data are presented in Table 5. All age uncertainties are given at the 2$\sigma$ level.

Selected grains for SHRIMP II analyses were mounted on epoxy discs with chips of the mineral standard, ground and polished until nearly half of each grain was removed, micro photographed in transmitted and reflected light, and imaged for their internal morphology using a scanning electron microscope (i.e. backscattered electrons). The mount was then cleaned and gold-coated to have a uniform electrical conductivity during the SHRIMP analyses. The standard used in the GSC laboratory is Kipawa zircon (993 Ma; $^{206}$Pb/$^{238}$U ratio = 0.16632), while the standards used at the UWA laboratory are Sri Lanka CZ3 zircon (564 Ma; $^{206}$Pb/$^{238}$U ratio = 0.0914), Khan titanite (518 Ma; $^{206}$Pb/$^{238}$U ratio = 0.083671), and Phalaborwa baddeleyite (2060 Ma; $^{206}$Pb/$^{238}$U ratio = 0.37652).

The isotopic composition of the minerals was determined using SHRIMP II (De Laeter and Kennedy, 1998) installed at Curtin University, using methods originally published by Compston et al. (1992) and more recently stated by Smith et al. (1998). For SHRIMP II analyses performed at the GSC the procedures are available in Stern (1997). Circular areas of 20–30 μm were analysed from morphologically distinct areas chosen within zircon grains, together with replicate analyses of the standard in the same epoxy mount. Corrections for common Pb were made using the measured $^{204}$Pb and the Pb isotopic composition of Broken Hill galena. For each spot analysis, the initial

60–90 s were used to rasterise and remove the gold, avoiding the analysis of common Pb from the coating. Results with more than 1% common lead correction were not used to calculate the ages: examples include grains a.15-1 and c.1-1 (Table 4). Data are plotted on concordia diagrams using ISOPLOT/Ex software (Ludwig, 1999) and error ellipses on concordia plots are shown at the 95% confidence level ($2\sigma$). All presented ages are weighted mean $^{207}Pb/^{206}Pb$ ages.

## References


Almeida, M.E., Brito, M.F.L., Macambira, M.J.B., 1999. Caroçal Granite: $^{207}Pb/^{206}Pb$ zircon evaporation age in post-collisional granitoids of Tapajós Gold Province, Amazonian region, Brazil. The Second South American Symposium on Isotope Geology, Cordoba, Argentina, pp. 3–6.

Almeida, M.E., Brito, M.F.L., Ferreira, A.C., 2000. Geologia da folha SB.21-V-D-Mamãe Anã. Projeto Tapajós. Companhia de Pesquisa de Recursos Minerais—CPRM. Rio de Janeiro, Brazil, 238 pp. (in Portuguese).

Almeida, M.E., Ferreira, A.L., Macambira, M.J.B., Sachett, C.R., 2001. Time constraint based on zircon dating for the Jacareacanga Group (Tapajós Province, Amazon Craton, Brazil). In: Tonlinson, A. (Ed.), The Third South American Symposium on Isotope Geology, Pucón, Chile. Comunicaciones, vol. 52, 26 pp.

Bahia, R., Quadros, M., 2000. Geologia da folha SB.21-X-C-Caracol. Projeto Tapajós. Companhia de Pesquisa de Recursos Minerais-CPRM, Rio de Janeiro, Brazil, 218 pp. (in Portuguese).

Basei, M.A.S., 1974. Estudo geocronológico do magmatismo ácido da região meridional da Amazônia. The 28th Congress on Bras. Geology, Porto Alegre, Brazil, pp. 287–296 (in Portuguese).

Basei, M.A.S., 1977. Idade do vulcanismo ácido-intermediário da região Amazônica. M.Sc. Thesis, Instituto de Geociências, University of São Paulo, São Paulo, Brazil (in Portuguese).

Bettencourt, J.S., Tosdal, R.M., Leite Jr, W.B., Payolla, B.L., 1999. Mesoproterozoic rapakivi granites of the Rondônia Tin Province, southwestern border of the Amazonian Craton, Brazil: I. Reconnaissance U–Pb geochronology and regional implications. Precambrian Res. 95, 41–67.

Bickford, M.E., Collerson, K.D., Lewry, J.F., Van Schmus, W.R., Chiarenzelli, J.R., 1990. Proterozoic collisional tectonism in the Trans-Hudson Orogen, Saskatchewan. Geology 18, 14–18.

Bizzinella, G.A., Santiago, A.F., Santos, A., Borges, F.R., Souza, F.J.C., Godoy, H.K., Yamaguti, H.S., Oliveira, J.R., Oliveira, L.R., 1980. Projeto Tapajós-Sucunduri, Relatório Final, partes I e II. Departamento Nacional da Produção Mineral, Companhia de Pesquisa de Recursos Minerais, Manaus, Brazil, vols. Ia and Ib (in Portuguese).

Boynton, W.V., 1984. Cosmochemistry of the rare earth elements: meteorite studies. In: Henderson, P. (Ed.), Rare Earth Element Geochemistry. Elsevier, Amsterdam.

Brito, M.F.L., Almeida, M.E., Ferreira, A.L., Monteiro, M.A.S., Popini, M.V.F., 1997. Petrografia e Litogeoquímica da Suíte Intrusiva Maloquinha—Registro de magmatismo tipo—A na Província do Tapajós. In: The Sixth Cong. Bras. Geoq., Salvador, Brazil, vol. 2, pp. 847–851 (in Portuguese).

Brown, G.C., 1982. Calc-alkaline intrusive rocks: their diversity, evolution, and relation to volcanic arcs. In: Thorpe, R.S. (Ed.), Orogenic Andesites and Related Rocks. Willey, London, pp. 437–461.

Brown, G.C., Thorpe, R.S., Webb, P.C., 1984. The geochemical characteristics of granitoids in contrasting arcs and comments on magma sources. J. Geol. Soc. Lond. 141, 413–426.

Compston, W., Williams, I.S., Kirschvink, J.L., Zichao, Z., Guogan, M., 1992. Zircon ages for the Early Cambrian timescale. J. Geol. Soc. Lond. 149, 171–184.

Costa, J.B.S., Hasui, Y., 1997. Evolução Geológica da Amazônia. In: Costa, M.L., Angelica, R.S. (Eds.), Contribuições à Geologia da Amazônia. Financiadora de Estudos e Projetos, Sociedade Brasileira de Geologia, Núcleo Norte, Belém, Brazil, pp. 15–90 (in Portuguese).

Coutinho, M.G.N., Santos, J.O.S., Fallick, A., Lafon, J.M., 2000. Orogenic gold deposits in Tapajós Mineral Province, Amazon, Brazil. In: The Thirty-first International Geological Congress, Rio de Janeiro, Brazil [CD-ROM].

Dall'Agnol, R., Costi, H.T., Leite, A.A.S., Magalhães, M.S., Teixeira, N.P., 1999. Rapakivi granites from Brazil and adjacent areas. Precambrian Res. 95, 9–39.

Davidson, A., Van Breemen, O., 1988. Baddeleyite–zircon relationships in coronitic metagabbro, Grenville Province, Ontario: implications for geochronology. Contrib. Mineral. Petrol. 1000, 291–299.

De Laeter, J.R., Kennedy, A.K., 1998. A double focusing mass spectrometer for geochronology. Int. J. Mass Spec. 178, 43–50.

Debon, F., Le Fort, P., 1983. A chemical-mineralogical classification of common plutonic rocks and associations. Trans. R. Soc. Edin. Earth Sci. 73, 135–149.

Faraco, M.T.L., Carvalho, J.M.A., Klein, E.L., 1996. Carta metalogenética da Província aurífera Tapajós, escala 1:500.000. Nota explicativa. Brazilian Geological Survey, Belém, Brazil, 13 pp. (in Portuguese).

Ferreira, E.O., 1959. Contribuição à litologia da Série Uatumã. Rio de Janeiro, Brazil. Boletim do Serviço Geol. Min. 185, 1–31 (in Portuguese).

Fraga, L.M.B., Almeida, M.E., Macambira, M.J.B., 1997. First lead–lead zircon ages of charnockitic rocks from Central Guiana Belt (CGB) in the State of Roraima, Brazil. The First South American Symposium on Isotope Geology, Campos do Jordão, 1997. Resumo, Campos do Jordão, São Paulo, pp. 115–117.

Gaudette, H.E., Olszewski Jr., W.J., 1985. Geochronology of the basement rocks, Amazonas Territory, Venezuela and the tectonic evolution of the western Guiana Shield. Geol. Mijnbouw 64, 131–143.

Geraldes, M.C., Van Schmus, W.R., Condie, K.C., Bell, S., Teixeira, W., Babinski, M., 2001. Proterozoic geologic evolution of the SW part of the Amazonian Craton in Mato Grosso state, Brazil. Precambrian Res. 111, 91–128.

Hartmann, L.A., Delgado, I.M., 2001. Cratons and orogenic belts of the Brazilian Shield and their contained gold deposits. Min. Deposita 36, 207–217.

Hoffman, P.F., 1988. United Plates of America, the birth of a continent: early Proterozoic assembly and growth of Laurentia. Ann. Rev. Earth Planet. Sci. 16, 543–603.

Jacobi, P.J., 2000. Technical reports. Reports on Tapajós Prospects. São Jorge. Available at: http://www.brasilvirtual.com/amazonexplorers/.

Klein, E.L., Vasquez, M., 2000. Geologia da folha SB.21-Z-A-Riozinho. Projeto Tapajós. Companhia de Pesquisa de Recursos Minerais-CPRM, Rio de Janeiro, Brazil, 240 pp. (in Portuguese).

Krogh, T.E., 1973. A low-contamination method for hydrothermal decomposition of zircon and extraction of U and Pb for isotopic age determinations. Geochem. Cosmochem. Acta 37, 485–494.

Krogh, T.E., 1982. Improved accuracy of U–Pb zircon ages by the creation of more concordant systems using an air abrasion technique. Geochim. Cosmochim. Acta 46, 637–649.

Lacerda Filho, J.V., Souza, J.O., Oliveira, C.C., Ribeiro, P.S.E., Vilas Boas, P.F., Albuquerque, M.C., Frasca, A.A.S., Borges, F.R., Moreton, L.C., Martins, E.G., Camargo, M.A., Valente, C.R., Pimentel, M.M., Botelho, N.F., 2001. Geologia e evolução tectônica da região norte de Mato Grosso. The Seventh Simpósio de Geologia da Amazônia, Belém, Brazil [CD-ROM], pp. 3–6 (in Portuguese).

Lamarão, C.N., Dall'Agnol, R., Lafon, J.M., Lima, E.F., 2002. Geology, geochemistry, and Pb–Pb zircon geochronology of the Paleoproterozoic magmatism of Vila Riozinho, Tapajós Gold Province, Amazonian Craton, Brazil. Precambrian Res. 119 (1–4), 189–223.

Lima, M.I.C., 1999. As subprovíncias da Província estrutural Amazônia. The Sixth Simpósio de Geologia da Amazônia, Manaus, Amazonas, pp. 259–262 (in Portuguese).

Ludwig, K.R., 1999. Using ISOPLOT/Ex, version 2: a geochronological toolkit for Microsoft Excel. Berkeley Geochronological Center Special Publication Ia, 47 pp.

Nardi, L.V.S., 1991. Caracterização Petrográfica e Geoquímica dos Granitos Metaluminosos da Associação Alcalina. Instituto de Geociências da UFRGS. Pesquisas 18 (1), 44–57 (in Portuguese).

Neder, R., Figueiredo, B.R., Beaudry, C., Collins, C., Leite, J.A.D., 2000. The Expedito massive sulfide deposit, Mato Grosso. Revista Brasileira de Geociências 30 (2), 222–225.

Nironen, M., 1997. The Svecoffenian Orogen: a tectonic model. Precambrian Res. 86, 21–44.

Parrish, R.R., Krogh, T.E., 1987. Synthesis and purification of $^{205}$Pb for U–Pb geochronology. Chem. Geol. 66, 103–110.

Parrish, R.R., Roddick, J.C., Loveridge, W.D., Sullivan, R.W., 1987. Uranium-lead analytical techniques at the Geochronology Laboratory, Geological Survey of Canada. In: Radiogenic Age and Isotopic Studies: Report 1. Geological Survey of Canada Paper 87-2, pp. 3–7.

Payolla, B.L., Bettencourt, J.S., Kozuch, M., Leite Jr., W.B., Fetter, A.H., Van Schmus, W.R., 2002. Geological evolution of the basement rocks in the east-central part of the Rondônia Tin Province, SW Amazonian Craton, Brazil: U–Pb and Sm–Nd isotopic constraints. Precambrian Res. 119, 141–169.

Pessoa, M.R., Santiago, A.F., Andrade, A.F., Nacimento, J.O., Santos, J.O.S., Oliveira, J.R., Lopes, R.C., Prazeres, W.V., 1977. Projeto Jamanxim. Relatório Final. Companhia de Pesquisa de Recursos Minerais, Departamento Nacional da Produção Mineral, Manaus, Unpublished Report, vols. 1–3 (in Portuguese).

Prazeres, W.V., Santos, A.J., Campos, M.J.F., Cavalcante, O.A., 1979. Projeto Estanho dos Granitos Maloquinha. Final Report. Departamento Nacional da Produção Mineral, Companhia de Pesquisa de Recursos Minerais, Manaus-Amazonas, vol. I-A, 301 pp. (in Portuguese).

Ricci, P.S.F., Vasquez, M.L., Santos, A., Klein, E.L., João, X.S.J., Martins, R.C., 1999. Suíte Intrusiva Creporizão-Província Tapajós: Proposta e critérios de definição. The Sixth Simpósio de Geologia da Amazônia, Manaus, Brazil, pp. 519–522 (in Portuguese).

Roddick, J.C., Loveridge, W.D., Parrish, R.R., 1987. Precise U–Pb dating of zircon at the sub-nanogram Pb level. Chem. Geol. 66, 111–121.

Rogers, J.J.W., 1996. A history of continents in the past three billion years. J. Geol. 104, 91–107.

Santos, D.B., Fernandes, P.E.C.A., Dreher, A.M., Cunha, F.M.B., Basei, M.A.S., Teixeira, J.B.G., 1975. Folha SB.21-Tapajós. Geologia. Projeto Radar na Amazônia, Departamento Nacional da Produção Mineral, Rio de Janeiro. Levantamento de Recursos Naturais 7, 15–116 (in Portuguese).

Santos, J.O.S., 1984. A parte setentrional do Cráton Amazônico (Escudo das Güianas) e a Bacia Amazônica. In: Schobbenhaus, C., Campos, D.A., Derze, G.R., Asmus, H.E. (Eds.), Geologia do Brasil, Departamento Nacional da Produção Mineral, Capítulo II, Brasília, pp. 57–88 (in Portuguese).

Santos, J.O.S., Reis Neto J.M., 1982. Algumas idades de rochas graníticas do Cráton Amazônico. The 32nd Congresso Brasileiro de Geologia, Salvador, Brazil, vol. 1, pp. 339–347 (in Portuguese).

Santos, J.O.S., Hartmann, L.A., Gaudette, H.E., 1997. Reconnaissance U–Pb in zircon, Pb–Pb in sulfides and review of Rb–Sr geochronology in the Tapajós Gold Province, Pará-Amazonas States, Brazil. In: Proceedings of the First South American Symposium on Isotope Geolology, Extended Abstracts, Campos do Jordão, Brazil, pp. 280–282.

Santos, J.O.S., Hartmann, L.A., Gaudette, H.E., Groves, D.I., McNaughton, N.J., Fletcher, I.R., 2000. A new understanding of the provinces of the Amazon Craton based on integration of field mapping and U–Pb and Sm–Nd geochronology. Gondwana Res. 3 (4), 453–488.

Santos, J.O.S., Groves, D.I., Hartmann, L.A., McNaughton, N.J., Moura, M.B., 2001. Gold deposits of the Tapajós and Alta Floresta domains, Tapajós–Parima orogenic belt, Amazon Craton, Brazil. Min. Deposita 36, 278–299.

Santos, J.O.S., Hartmann, L.A., McNaughton, N.J., Fletcher, I.R., 2002. Timing of mafic magmatism in Tapajós Province and implications for the evolution of the Amazon Craton: evidence from baddeleyite and zircon U–Pb SHRIMP geochronology. J. S. Am. Earth Sci. 15, 409–429.

Santos, J.O.S., Hartmann, L.A., Bossi, J., Campal, N., Schipilov, A., Piñeyro, D., McNaughton, N.J., 2003a. Duration of the Trans-Amazonian Cycle and its correlation within South

America based on U–Pb SHRIMP geochronology of the La Plata Craton, Uruguay. Int. Geol. Rev. 45 (1), 27–48.

Santos, J.O.S., Potter, P.E., Reis, N.J., Hartmann, L.A., Fletcher, I.R., McNaughton, N.J., 2003b. Age, source and regional stratigraphy of the Roraima Supergroup and Roraima-like outliers in northern South America based on U–Pb geochronology. Geol. Soc. Am. Bull. 115 (3), 331–348.

Silva, G.H., Leal, J.W.L., Montalvão, R.M.G., Bezerra, P.E.L., Pimenta, O.N.S., Tassinari, C.C.G., Fernandes, P.E.C.A., 1980. Geologia, In: Folha SC.21-Juruena: geologia, geomorfologia, pedologia, vegetação e uso potencial da terra. Rio de Janeiro: Departamento Nacional da Produção Mineral. Projeto Radar na Amazônia Brasil, pp. 21–116 (in Portuguese).

Smith, J.B., Barley, M.E., Groves, D.I., Krapez, B., McNaughton, N.J., Bickle, M.J., Chapman, H.J., 1998. The Scholl shear zone, West Pilbara: evidence for a terrane boundary structure from integrated tectonic analyses, SHRIMP U–Pb dating and isotopic and geochemical data of granitoids. Precambrian Res. 88, 143–171.

Stacey, J.S., Kramers, J.D., 1975. Approximation of terrestrial lead isotope evolution by a two stage model. Earth Planet. Sci. Lett. 26, 207–221.

Steiger, R.H., Jäger, E., 1977. Subcommission on geochronology: convention on the use of decay constants in geo- and cosmochronology. Earth Planet. Sci. Lett. 36, 359–362.

Stern, R.A., 1997. The GSC sensitive high resolution ion microprobe (SHRIMP): analytical techniques of zircon U–Th–Pb age determinations and performance evaluation. In: Radiogenic Age and Isotopic Studies: Report 10. Geol. Surv. Can. Curr. Res. 1997-F, 1–31.

Stern, R.A., Syme, E.C., Bailes, A.H., Lucas, S.B., 1995. Paleoproterozoic (1.90–1.86 Ga) arc volcanism in the Flin Flon Belt, Trans-Hudson Orogen, Canada. Contrib. Mineral. Petrol. 119, 117–141.

SUDAM-Superintendência para o Desenvolvimento da Amazônia, 1972. Geologia básica, prospecção geoquímica e por concentrados de bateia na região dos rios Tapajós e Maués. GEOMITEC, Superintendência para o Desenvolvimento da Amazônia, Belém, vol. 2, 281 pp. (in Portuguese).

Tassinari, C.C.G., 1996. O mapa geocronológico do Cráton Amazônico no Brasil: Revisão dos dados isotópicos. Post-Doctoral Thesis, Instituto de Geociências, University of São Paulo, São Paulo, Brazil, 139 pp. (in Portuguese).

Tassinari, C.C.G., Macambira, J.B.M., 1999. Geochronologial provinces of the Amazonian Craton. Episodes 22 (3), 174–182.

Tassinari, C.C.G., Bettencourt, J.S., Geraldes, M.C., Macambira, J.B.M., Lafon, J.M., 2000. The Amazonian Craton. In: Cordani, U.G., Milani, E.J., Thomaz Filho, A., Campos, D.A. (Eds.), Tectonic Evolution of South America. The Thirty-first International Geological Congress, Rio de Janeiro, 2000, pp. 41–96.

Thiéblemont, D., Tégyey, M., 1994. Une discrimination géochimique des roches différenciés témoin de la diversité d'órigine et de situation tectonique des magmas calco-alcalins. C. R. Acad. Sci. Paris 319 (2), 87–94.

Väisänen, M., Mänttäri, I., Hölttä, P., 2002. Svecofennian magmatic and metamorphic evolution in southwestern Finland as revealed by U–Pb zircon SIMS geochronology. Precambrian Res. 116, 111–127.

Van Kranendonk, M.J., St-Onge, M.R., Henderson, J.R., 1993. Paleoproterozoic tectonic assembly of Northeast Laurentia through multiple indentations. Precambrian Res. 63, 325–347.

Van Schmus, W.R., Bickford, M.E., Lewry, J.F., MacDonald, R., 1987. U–Pb geochronology in the Trans-Hudson Orogen, northern Saskastchewan, Canada. Can. J. Earth Sci. 24, 407–424.

Vasquez, M.L., Klein, E., 2000. Projeto Especial Província Mineral Tapajós. Geologia e recursos minerais da Folha Rio Novo-SB.21-Z-C, Estado do Pará, Escala 1:250.000, Companhia de Pesquisa de Recursos Minerais, Brasília, Brazil, [CD-ROM] (in Portuguese).

Wingate, M.T.D., Compston, W., 2000. Crystal orientation effects during ion microprobe U–Pb analysis of baddeleyite. Chem. Geol. 168 (1/2), 75–97.